



Contents lists available at ScienceDirect

Deep-Sea Research II

journal homepage: www.elsevier.com/locate/dsr2

Western Ross Sea continental slope gravity currents

Arnold L. Gordon^{a,*}, Alejandro H. Orsi^b, Robin Muench^c, Bruce A. Huber^a,
Enrico Zambianchi^d, Martin Visbeck^e^a Lamont-Doherty Earth Observatory, Palisades, NY 10964, USA^b Department of Oceanography, Texas A&M University, College Station, TX 77843-3146, USA^c Earth and Space Research, 2101 Fourth Avenue, Suite 1310, Seattle, WA 98121, USA^d Dipartimento di Scienze per l'Ambiente, Università degli Studi di Napoli "Parthenope" Centro Direzionale, Isola C4, 80143 Napoli, Italy^e Leibniz-Institut für Meereswissenschaften (IFM-GEOMAR), Düsternbrooker Weg 20, D-24105 Kiel, Germany

ARTICLE INFO

Article history:

Accepted 24 October 2008

Available online 7 December 2008

Keywords:

Ross Sea

Southern Ocean

Water masses

Oceanic boundary layer

Oceanic fronts

Oceanic currents

ABSTRACT

Antarctic Bottom Water of the world ocean is derived from dense Shelf Water that is carried downslope by gravity currents at specific sites along the Antarctic margins. Data gathered by the AnSlope and CLIMA programs reveal the presence of energetic gravity currents that are formed over the western continental slope of the Ross Sea when High Salinity Shelf Water exits the shelf through Drygalski Trough. Joides Trough, immediately to the east, offers an additional escape route for less saline Shelf Water, while the Glomar Challenger Trough still farther east is a major pathway for export of the once supercooled low-salinity Ice Shelf Water that forms under the Ross Ice Shelf. The Drygalski Trough gravity currents increase in thickness from ~100 to ~400 m on proceeding downslope from ~600 m (the shelf break) to 1200 m (upper slope) sea floor depth, while turning sharply to the west in response to the Coriolis force during their descent. The mean current pathway trends ~35° downslope from isobaths. Benthic-layer current and thickness are correlated with the bottom water salinity, which exerts the primary control over the benthic-layer density. A 1-year time series of bottom-water current and hydrographic properties obtained on the slope near the 1000 m isobath indicates episodic pulses of Shelf Water export through Drygalski Trough. These cold (< -1 °C), salty (> 34.75) pulses correlate with strong downslope bottom flow. Extreme examples occurred during austral summer/fall 2003, comprising concentrated High Salinity Shelf Water (-1.9 °C; 34.79) and approaching 1.5 m s⁻¹ at descent angles as large as ~60° relative to the isobaths. Such events were most common during November–May, consistent with a northward shift in position of the dense Shelf Water during austral summer. The coldest, saltiest bottom water was measured from mid-April to mid-May 2003. The summer/fall export of High Salinity Shelf Water observed in 2004 was less than that seen in 2003. This difference, if real, may reflect the influence of the large iceberg C-19 over Drygalski Trough until its departure in mid-May 2003, when there was a marked decrease in the coldest, saltiest gravity current adjacent to Drygalski Trough. Northward transport of cold, saline, recently ventilated Antarctic Bottom Water observed in March 2004 off Cape Adare was ~1.7 Sv, including ~0.4 Sv of High Salinity Shelf Water.

© 2008 Published by Elsevier Ltd.

1. Introduction

Dense water formed through water-mass modification along the Antarctic margins spreads over the global ocean seafloor as Antarctic Bottom Water (AABW; Orsi et al., 1999). Approximately, 80% of the deep seafloor is blanketed by water colder than 1 °C, which is too cold to be derived from North Atlantic Deep Water and must have its origins as AABW. Johnson (2008), utilizing the seawater properties of AABW and NADW, estimates that the ratio

of AABW volume to that of NADW is about 1.7, with AABW covering more than twice the area of the sea floor than does NADW. AABW gains heat, as it spreads away from Antarctica, through mixing with ambient waters. Eventually, the more buoyant product returns to the Southern Ocean as upwelling Circumpolar Deep Water, thus closing the lower limb of the global Southern Ocean Meridional Overturning Circulation (MOC).

Deep-water inventories of chlorofluorocarbon (CFC) data (Orsi et al., 1999, 2001, 2002) provide estimates of the transports and ventilation rates associated with water-mass modifications and subsequent overturning processes along the Antarctic continental margin; see Fig. 5 in Orsi et al. (2002). Orsi et al. (2002) find that the sum of Southern Ocean surface and shelf water entering into

* Corresponding author.

E-mail address: agordon@ldeo.columbia.edu (A.L. Gordon).

the deep- and bottom-water stratum is 13.7 Sv ($1 \text{ Sv} = 10^6 \text{ m}^3 \text{ s}^{-1}$), comprised of 5.4 ± 1.7 Sv of dense shelf water and 4.7 Sv of offshore CFC-enriched surface water that descends over the continental slope, and 3.6 ± 1.3 Sv of CFC-enriched surface water that descends into the upper deep water within the circumpolar zone well offshore of the Antarctic margin. Mixing of the 5.4 Sv shelf water, with 4.7 Sv of offshore surface water and 7.4 Sv of CFC-poor lower Circumpolar Deep Water over the slope delivers 8.1 Sv into the bottom layer (>2500 m) and 9.4 Sv into the deep layer (1500–2500 m). The 17.5 Sv sum of these volume fluxes, plus the 3.6 Sv of descending offshore surface waters, totals 21 Sv, exceeding the CFC inventory-based estimate of 17 Sv for North Atlantic Deep Water formation (Smethie and Fine, 2001). LeBel et al., 2008. Analysis of the 1970–1997 CFC data arrive at an NADW formation rate of 19.6 Sv, effectively the same as the southern ocean ventilation value.

While global in extent, AABW forms initially through small-scale, energetic processes associated with the ~ 5.4 Sv export of dense Antarctic Shelf Water and subsequent entrainment of ambient slope water (Orsi et al., 2001). Shelf Water is not exported uniformly around Antarctica, but rather at a limited number of shelf localities where substantial buoyancy loss leads to formation of dense water and, in turn, to a variety of AABW types (Gordon, 1974). Virtually all of these localities are situated in the Weddell and Ross seas, and along the Adélie Coast and Prydz Bay regions (Foster, 1995; Baines and Condie, 1998; Whitworth et al., 1998; Gordon, 1998; Rintoul, 1998; Orsi et al., 1999; Foldvik et al. 2004; Jacobs, 2004).

Descent of dense water over the continental slope is usually referred to as a gravity current, a density current or a cascade (Ivanov et al., 2004; Legg et al., 2009). Gravity currents are instrumental in forming and modifying deep-ocean water masses, both in the Southern Ocean and at northern hemisphere sites. Examples situated outside the Antarctic include overflows from the Nordic seas (Girton and Sanford, 2003; Saunders, 1990) leading to the formation of the densest form of NADW, and from the subtropical marginal seas of the Mediterranean (Price et al., 1993; Price and Baringer, 1994) and Red Sea (Peters et al., 2005).

Small spatial and temporal scales are associated with gravity currents, where the internal deformation radius (R_0) can be only a few kilometers. Their interactions with ambient water and bottom roughness, the steering influence of local sea floor morphology, and the effects of oscillatory tidal currents all contribute significant challenges for both observationally based research and for effective parameterization of gravity currents within large-scale ocean models (Baines and Condie, 1998; Tanaka and Akitomo, 2001; Özgökmen et al., 2004; Ou, 2005; Xu et al., 2006; Legg et al., 2009). The harsh polar environmental conditions and small R_0 (~ 5 km) make the processes involved with the export of Antarctic Shelf Water especially difficult to adequately document.

This paper seeks to provide an observationally based, regional description of the gravity current stratification and velocity characteristics over the continental slope of the western Ross Sea region. We focus on export of saline Shelf Water through the Drygalski Trough. We utilize the stratification and shear data gathered by the AnSlope austral summer/fall cruises of 2003 and 2004; the AnSlope current and temperature/salinity mooring time series 2003–2005; and the austral summer 2003 CLIMA stratification observations.

The regional scale is loosely defined here as $2R_0$ (~ 10 km). Strong tides typify the Ross Sea (Padman et al., 2003, 2009; Erofeeva et al., 2005) and are fundamental in governing the timing of export of Shelf Water (Whitworth and Orsi, 2006; Padman et al., 2009; Muench et al., 2008). Localized topography, such as canyons at the <5 km scale that are not well resolved by the AnSlope data set, also might influence gravity currents. Other

papers in this issue, e.g. Visbeck and Thurnherr (2009), discuss aspects of such small-scale features. Presentation of the AnSlope tracer data is in preparation for future publication, and will not be addressed here. For a comprehensive assessment of the general Ross Sea oceanography and water-mass nomenclature, the reader is referred to Orsi and Wiederwohl (2009), and to papers by Jacobs (e.g. Jacobs et al., 1970, 1985; Smethie and Jacobs, 2005). The Antarctic Slope Front (Jacobs, 1991; Whitworth et al., 1998) of the Ross Sea is being addressed in an ongoing effort. Gordon et al. (2004) present a preliminary assessment of the gravity currents observed using the AnSlope 2003 data.

2. AnSlope and CLIMA

The 2003–2005 AnSlope program in the Ross Sea had as a goal the identification and quantification of the principal physical processes governing (1) the transfer of dense Antarctic Shelf Water into intermediate and deep layers of the adjacent deep ocean and (2) the compensatory poleward flow of warmer and less-dense open-ocean waters across the shelf break. Selection of the northwest Ross Sea as the study site was based on its previous identification as a primary site for significant outflow of dense Antarctic Shelf Water (Jacobs et al., 1970, 1985; Gordon, 1974). The region further provides all the ingredients for an investigation of the underlying physical mechanisms, yet in an environment of greater accessibility than that of other Antarctic deep water formation sites such as the western Weddell Sea shelf. The central and western Ross Sea shelf is cut by three major north–south-oriented topographic troughs, each inducing dips in the sill of the outer shelf (Fig. 1A). From west to east, they are as follows: Drygalski Trough, sill depth 510 m; Joides Trough, sill depth of 510 m; and Glomar Challenger Trough, sill depth 570 m (Smith and Sandwell, 1997; url: http://topex.ucsd.edu/marine_topo/).

AnSlope field studies consisted of three cruises on the research icebreaker Nathaniel B. Palmer during which detailed observations were made of water-column characteristics. The measurements included temperature, salinity, oxygen (CTD/ O_2), and chemical tracers: CFC-11, 12, 13, tritium and deuterium (analysis of water samples) and current shear (lowered acoustic Doppler current profiler (LADCP)). These expeditions took place from February to April 2003 and 2004 and from November to December 2004 (Fig. 1A; not shown in this figure are the October 2004 CTD stations made off Adélie Land).

The AnSlope moorings (Table 1, map view given in Fig. 5) were initially deployed in March 2003. These were recovered in March 2004 and a subset was redeployed for another year with final recovery in February 2005. Moored instruments deployed during AnSlope were positioned at depths deemed sufficient to protect the instruments from collision with iceberg keels; therefore, no time-series current observations were obtained shallower than ~ 400 m on the continental slope. Mooring blowdown of up to several hundred meters occurred, particularly on the upper slope, due to spring tidal currents that approached 1.5 m s^{-1} and had corresponding cross-slope excursions nearing 20 km (Whitworth and Orsi, 2006; Padman et al., 2009). These extreme excursions led both to short-term lateral advection and to high rates of ship drift during occupation of oceanographic stations. Potential impacts of the tidal effects on sampling are addressed where appropriate in the data presentation.

The Italian Climate Long-term Interaction of the Mass balance of Antarctica (CLIMA) project, started in 1994, provided the general framework in which physical oceanographic activities within the Italian National Program for Antarctic Research (PNRA) have been carried out (Fig. 1B). Over this period, six extensive oceanographic cruises have been organized in the central and

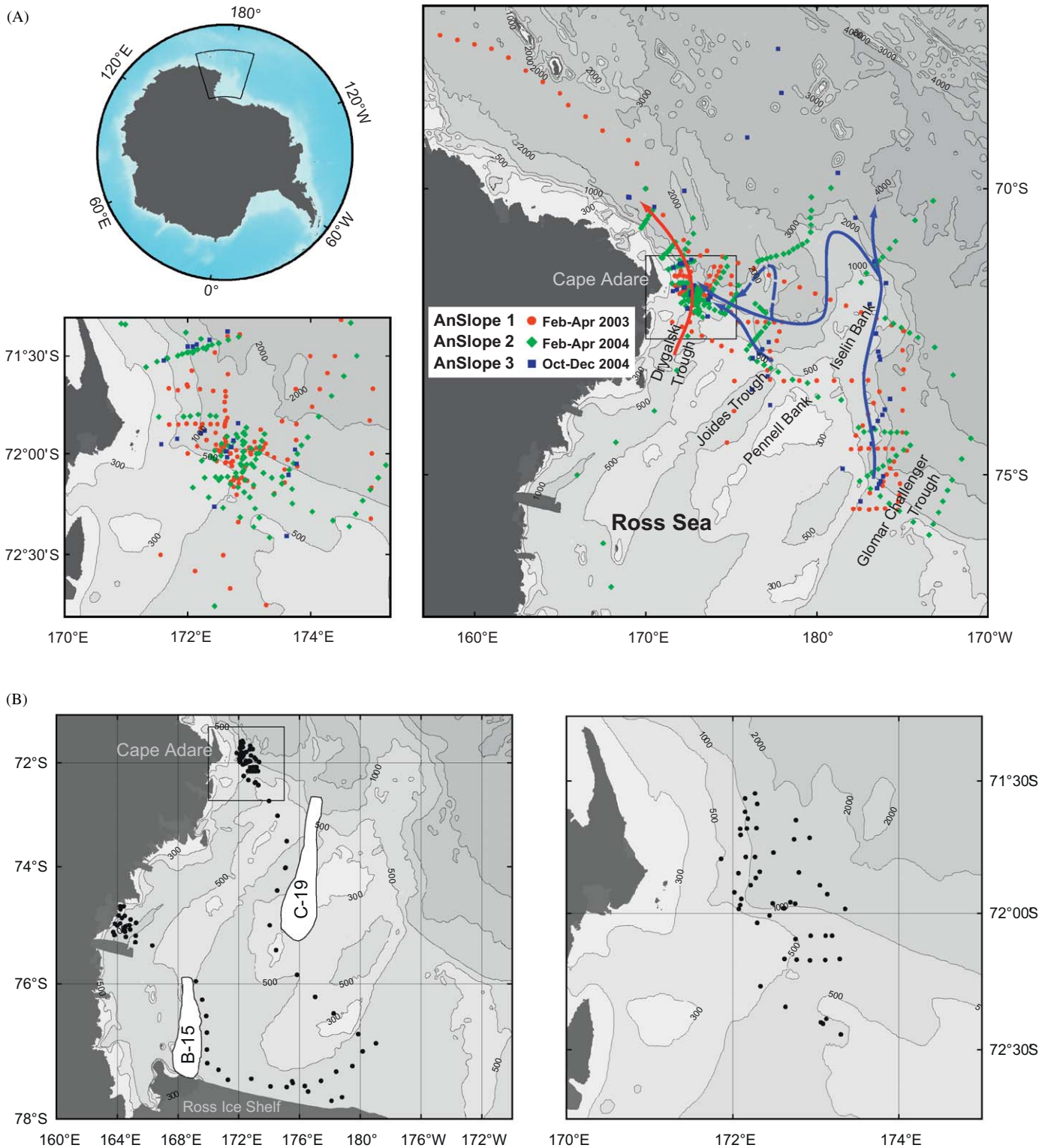


Fig. 1. (A) Distribution of AnSlope CTD/LADCP stations, color coded for each of the three AnSlope cruises. The arrows on the map show the bottom circulation patterns as determined from the CTD/LADCP data: red arrow shows the outflow of saline shelf water from the Drygalski Trough; the blue arrows show the flow of less saline water derived from the Joides Trough and from the Glomar Challenger Trough. (B) CLIMA CTD stations obtained in December 2002 and January 2003. Left panel shows all CTD stations (the positions of icebergs B-15 and C-19 in January 2003 are indicated); right panel shows the stations within the box shown on the left panel off Cape Adare (for interpretation of the references to color in this figure legend, the reader is referred to the web version of this article).

western Ross Sea from the Ross Ice Shelf margin across the shelf-break and to the lower slope. An overview of the variability of hydrological properties in the Ross Sea as revealed by the 12-year CLIMA data set is being addressed in an ongoing effort (Budillon, 2008 personal communication). In addition to collecting hydro-

graphic data, oxygen, nutrients, and chemical tracers were acquired during these cruises. Over the same period CLIMA deployed and maintained six moorings equipped with current meters, temperature and salinity recorders and sediment traps. From its initial focus on water-mass formation in the area of the

Table 1
AnSlope moored arrays.

<i>CENT-A</i>			
172°57.24'E	72°9.7'S	505 m	
MCat	273	CTP	
RCM	377	UVTP	
RCM	484	UVT	
MCat	494	CT	
<i>CENT-B1</i>			
173°6.16'E	72°3.84'S	549 m	
MCat	304	CTP	
RCM	404	---TP	
RCM	524	UVT	
Scat	533	CTP	
<i>CENT-B2</i>			
172°56.5'E	72°5.68'S	525 m	
MCat	281	CTP	
RCM	381	UVT	
RCM	502	---T	
Scat	512	CTP	
<i>CENT-C</i>			
173°5.57'E	72°1.84'S	651 m	
MCat	349	CTP	
RCM	449	UVTP	
RCM	551	UVTP	
RCM	630	UVT	
MCat	639	CT	
<i>CENT-D</i>			
173°11.45'E	71°58.89'S	1118 m	
MCat	403	CTP	
RCM	508	UVTP*	
RCM	716	UV*TP	
MCat	910	CTP*	
RCM	1097	---T	
MCat	1107	CT	
<i>CENT-E1</i>			
173°12.75'E	71°57.25'S	1407 m	
MCat	107	CTP	
RCM	207	UVTP	
RCM	407	UVTP	
MCat	707	CTP	
RCM	1007	UVTP	
MCat	1207	CTP	
RCM	1387	UVT	
MCat	1397	CT	
<i>CENT-E2</i>			
173°12.69'E	71°54.83'S	1772 m	
MCat	354	CTP	
RCM	461	UVTP	
RCM	677	UV*TP	
MCat	965	CTP	
RCM	1266	---T	
MCat	1468	CTP	
RCM	1751	UVT	
MCat	1761	CT	
<i>WEST-A</i>			
172°49.58'E	72°00.60'S	609 m	
RCM	419	UVTP	
RCM	520	-----	
RCM	587	UV*T	
MCat	597	CTP	
<i>WEST-B</i>			
172°45.42'E	71°58.20'S	1025 m	
RCM	432	UVTP	
RCM	632	UV*TP	

Table 1. (continued)

MCat	828	CTP*	
RCM	1004	UVT	
MCat	1014	CT	
<i>WEST-C</i>			
172°43.64'E	71°56.33'S	1630 m	
RCM	436	---TP	
RCM	629	---TP	
MCat	923	CTP*	
RCM	1238	UVTP	
MCat	1428	CTP*	
RCM	1609	UVT	
MCat	1619	CT	
<i>EAST-A</i>			
173°35.16'E	72°07.71'S	597 m	
Not recovered			
<i>EAST-B</i>			
173°37.69'E	72°03.84'S	982 m	
RCM	367	---TP*	
RCM	586	UVTP	
RCM	961	UVT	
MCat	971	CT	
<i>ADP-1</i>			
172°35.68'E	71°58.88'S	890 m	
MCat	731	CTP	
MCat	809	CTP	
MCat	872	CTP	
Steck	878	UVP*	
<i>PG-1</i>			
173°34.70'E	72°07.22'	629 m	
Mcat	629	CTP	
<i>M1</i>			
172°41.72'E	72°5.81'S	498 m	
MCat	247	CT	
RCM	248	UVTP	
MCat	397	CTP	
RCM	398	UVT-	
RCM	478	UVT-	
MCat	488	CT	
<i>M2</i>			
173°3.99'E	72°3.66'S	541 m	
Not recovered			
<i>M3</i>			
173°0.04'E	72°0.15'S	691 m	
MCat	390	CTP	
RCM	391	UVT-	
MCat	490	CTP	
RCM	491	UVT-	
MCat	591	CT	
RCM	671	---T	
MCat	681	CT	
<i>M4</i>			
172°55.02'E	71°58.67'S	984 m	
MCat	383	CTP	
RCM	384	UVTP	
MCat	583	CTP	
RCM	584	---T-	
MCat	783	CTP	
RCM	784	UVTP*	
RCM	964	UVT	
MCat	974	CT	
<i>M5</i>			

Table 1. (continued)

172°55.33'E	71°54.43'S	1749 m
MCat	448	CTP
RCM	449	UVTP
MCat	648	CT
RCM	649	--T
MCat	1048	CTP
RCM	1049	UVTP
MCat	1548	CTP*
RCM	1549	--T
RCM	1729	UVT
MCat	1739	CT
ADP-2		
172°53.97'E	72°3.98'S	529 m
MCat	512	CTP
MC	517	CT
Steck	517	

Mooring; position, water depth; instrument, nominal depth, data return. Measurements are of east–west (U) and north–south (V) currents, conductivity (C), temperature (T), and pressure (P). All Rotor Current Meters (RCM) were furnished with T sensors, and all MicroCat (MCat) recorders had C and T sensors; whereas only a subset of the RCMs and MCats has P sensors. Some data (–) were entirely lost consequent to malfunction or damage; and some data (*) were compromised by mooring blow-over due to strong total currents, or had gaps, or were suspected of problems. The first array (Central, West, East, ADP-1, PG-1) was deployed March 1–6, 2003 and recovered February 26–28, 2004. Moorings Central B and E were recovered and repositioned on 24–25 March 2003. The second yearlong array (M1–M5, ADP-2) was deployed March 6–10, 2004 and recovered February 2–3, 2005.

Terra Nova Bay Polynya, the research objectives of CLIMA have been broadened to encompass the formation and spreading processes of shelf waters originated in the central and western Ross Sea up to their overflow across the shelf break into the deeper regions of the Southern Ocean.

In addition to exchange of scientific personnel between the two projects, in 2003, the synergy between CLIMA and AnSlope led to organization of two coordinated oceanographic cruises which covered the same region in the western Ross Sea in subsequent periods: the CLIMA expedition onboard the R/V *Italica* from mid-January to the end of February, followed by the AnSlope1 voyage from the end of February to early April of 2003. Fig. 1B shows the distribution of the 2003 CLIMA CTD station network.

3. Regional thermohaline stratification

The regional temperature and salinity stratification observed during late austral summer–early fall 2003 and 2004 is shown in Fig. 2.

As typical for the ocean south of the Antarctic Circumpolar Current, the thermohaline stratification is composed of cold, relatively low-salinity surface and bottom layers with a warmer and more saline intervening deep layer. The temperature and salinity ranges vary with location. Over the Ross Sea continental slope, roughly deeper than 600 m, the transition from relatively warm deep water to cold bottom water is abrupt and forms a distinct transition layer separating the benthic boundary layer, which marks the gravity current, from the overlying ambient waters. Temperatures in this benthic layer fall primarily in the -0.5 to -1.0 °C range.

3.1. Continental slope stratification

Over the slope the potential temperature maximum θ_{\max} at 1.0 – 1.5 °C between 250 and 450 m marks the core of the regional circumpolar deep water (CDW). Potential temperatures <0 °C

within ~ 500 m of the sea floor mark the presence of Shelf Water within the benthic layer. In the eastern end of the AnSlope CTD survey region, the CDW layer was ~ 0.5 °C warmer than to the west near Cape Adare (red symbols in Fig. 2A and C). This warming reflects the larger-scale cyclonic Ross Sea gyre, which brings warm CDW into the Ross Sea from the northeast (see the 28.05 neutral density surface in Fig. 13 of Orsi and Wiederwohl, 2009; Orsi and Whitworth, 2004). En route mixing and heat loss upon exposure to the cooler waters exiting the continental margins gradually attenuate these higher temperatures. At and below the CDW θ_{\max} the relatively abrupt shift of the θ/S trend towards lower salinity adjacent to Joides Trough, relative to that east of Iselin Bank (Fig. 2A and C) suggests inhibition by Iselin Bank of the westward flow of warmer, saltier open-ocean CDW brought into the region by the cyclonic Ross Sea Gyre. This may have a bearing on the final form of the AABW emanating from the western Ross Sea.

The CDW salinity maximum S_{\max} is deeper than θ_{\max} , being closer to 600–900 m. It too shows a progressive decrease in CDW core values towards the west, with a relatively abrupt shift across Iselin Bank. As the sea floor is approached in the eastern regions, salinity decreases within the benthic layer. However, in the western sections (orange and red symbols, Fig. 2) the opposite is true, and delta salinity (the difference between the observed salinity relative to a linear fit in θ/S space from θ_{\max} to Ice Shelf Water (ISW) is positive. At some stations, the bottom salinity exceeds that of the CDW S_{\max} . This, as discussed below, is due to the export of a particularly saline form of freezing point Ross Sea Shelf Water that is referred to as High Salinity Shelf Water (HSSW) and is exported to the continental slope by way of the Drygalski Trough.

3.2. Continental shelf stratification

Water on the continental shelf is near the sealevel pressure freezing point of ~ -1.93 °C within the surface and benthic layers. At some sites, the temperature is below -2.0 °C between 200 and 450 m. These low temperatures are associated with ISW (best seen on the CLIMA continental shelf stations, Fig. 2B) that has formed at depth and correspondingly elevated pressures along the base of the Ross Ice Shelf farther south. There, open-ocean Shelf Water formed at the sea surface, with temperature at the surface pressure freezing point, flows under the ice shelf where, upon melting of basal glacial ice at elevated pressure, it is further cooled to the in situ freezing point (Lusquinos, 1963), which can be significantly less than -2 °C. There are two θ/S -defined locations of ISW, one centered at a salinity of 34.62 and the other at 34.75 (Fig. 2B). The former is produced under the main Ross Ice Shelf (Jacobs et al., 1970), while the latter forms within Terra Nova Bay through interaction with the Drygalski Ice Tongue (Kurtz and Bromwich, 1983, 1985; Van Woert, 1999; Budiillon and Spezie, 2000).

Due to the thermobaric effect (McDougall, 1987; McPhee, 2003), low ISW temperatures may play a central role in the formation and dynamics of gravity currents. Cold water, being more compressible than warmer water, is more apt to sink to deeper levels as increased pressure increases the density of the descending cold water, effectively providing a positive feed-back to the descent. This thermobaric effect may be particularly critical at the Glomar Challenger Trough, where cold ISW occurs in higher concentrations than at the Drygalski Trough (Bergamasco et al., 2002). The thermobaric effect has been investigated for open-ocean convection by McPhee (2003), but its relative role in gravity currents, while suggested (Legg et al., 2009), requires further evaluation.

From 200 to 500 m depths over the continental shelf a θ_{max} marks the core of the modified CDW (MCDW), which is formed when CDW mixes with ambient shelf water as it spreads southward onto the shelf. The MCDW θ_{max} is coldest, $< -1^\circ\text{C}$, over the inner shelf, with a salinity between 34.4 and 34.5. At the shelf break, closer to its source, the MCDW θ_{max} approaches that of the slope regime, with salinity of > 34.6 .

Shelf Water salinity spans the full salinity range of the entire region. The surface water is lowest in salinity, but the sub-surface water salinities vary from low-salinity Shelf Water (LSSW, < 34.6), ISW water (34.62 and 34.75), and HSSW characteristic of the Ross Sea (> 34.7 and as high as > 34.85) (Fig. 2B, Orsi and Wiederwohl, 2009). This wide salinity range of near-freezing water offers a broad range of densities, given the dominant salinity control over density at near-freezing temperatures, with a subsequently broad range of impacts on the derived benthic layers and deep-ocean AABW characteristics.

3.3. Summer 2003/summer 2004 differences

Comparison between the summer stratification observed in 2004 and that observed in 2003 reveals differences, though these may stem in part from the variation in CTD sampling patterns.

More θ/S data points were measured during 2004 than in 2003 in the deeper levels of CDW, below 0°C , with slightly lower salinity than observed in 2003. Although this difference may in part be a consequence of a greater concentration of CTD stations in 2004 than 2003 on the slope off Drygalski Trough, comparison of the orange coded section of both years (Fig. 2A and C) indicate a shift of θ/S points towards lower salinity in 2004. This is consistent with differences observed in the export of the HSSW: more in austral summer 2003, less in austral summer 2004, as discussed below.

4. Bottom-water properties

The distribution of θ and S through the lower 20 m of the water column over the outer shelf and slope (Fig. 3) reveals spatial patterns in the benthic-layer thermohaline composition. Over the continental slope east of the Glomar Challenger Trough, bottom water was relatively warm and salty (0.5°C , 34.69), with a marked shelf-break transition from the colder, fresher bottom water on the shelf. Slope bottom-water cooled and freshened (-0.5°C , 34.67) toward the north along the eastern flank of Iselin Bank, consistent with export of colder Shelf Water from the Glomar Challenger Trough (Bergamasco et al., 2002). Much of this bottom

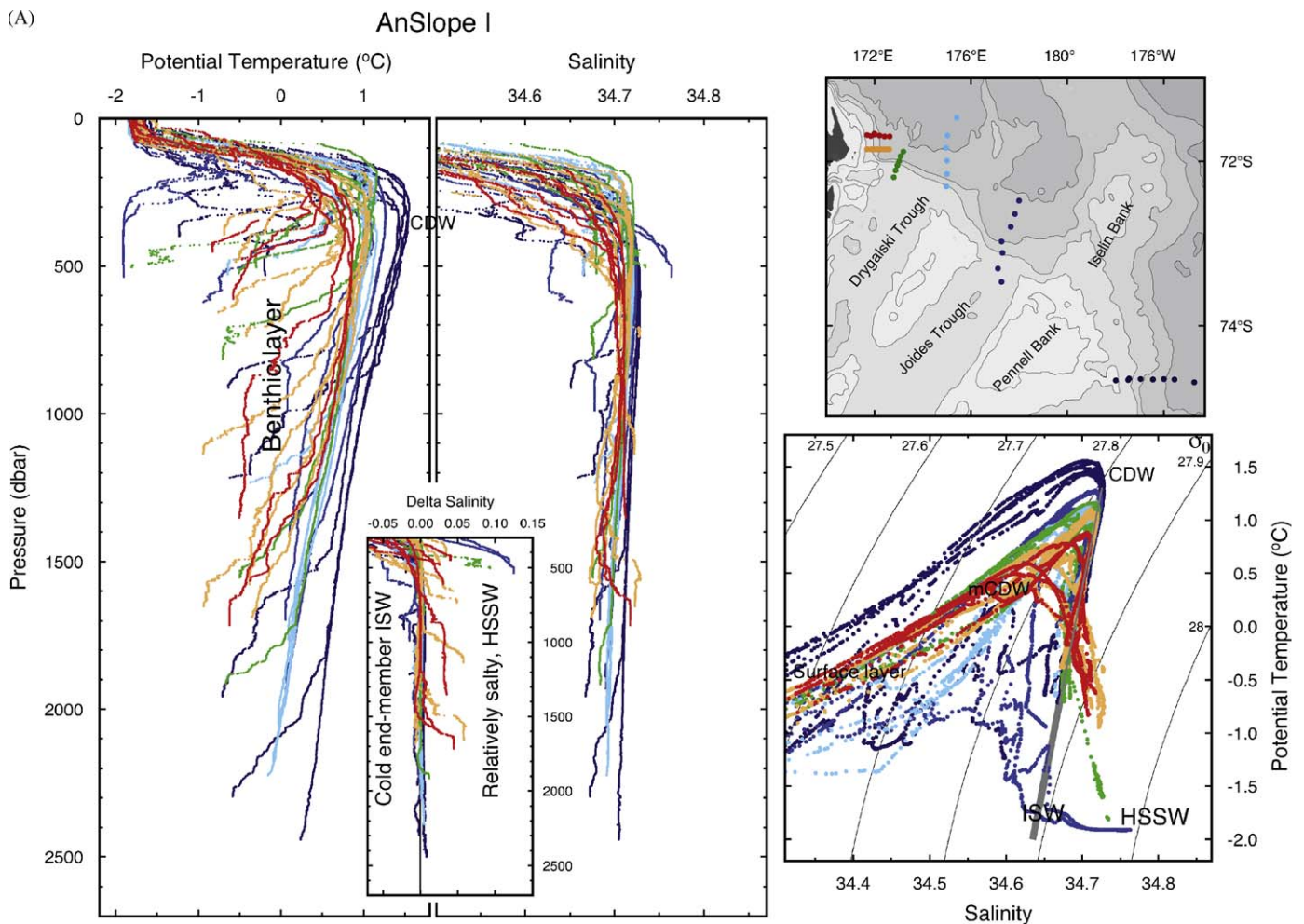


Fig. 2. (A) Potential temperature (θ $^\circ\text{C}$) and salinity (S) stratification and θ/S properties at six transects over the shelf/slope transition from February to April 2003. The sections are color coded from blue to red on progressing westward from Glomar Challenger Trough to Cape Adare, as shown on the inset map. To better display the variability of benthic layer salinity relative to the deep water, the central panel shows the salinity relative to a linear fit as shown on the θ/S scatter from the circumpolar deep water to the Ross Ice Shelf Water at a salinity 34.62. (B) Potential temperature (θ $^\circ\text{C}$) and salinity (S) stratification and θ/S properties within the western Ross Sea in January 2003 (from CLIMA). The stations are colored coded for position as indicated in the inset map. (C) Same as Fig. 2A, except for summer 2004 (for interpretation of the references to color in this figure legend, the reader is referred to the web version of this article).

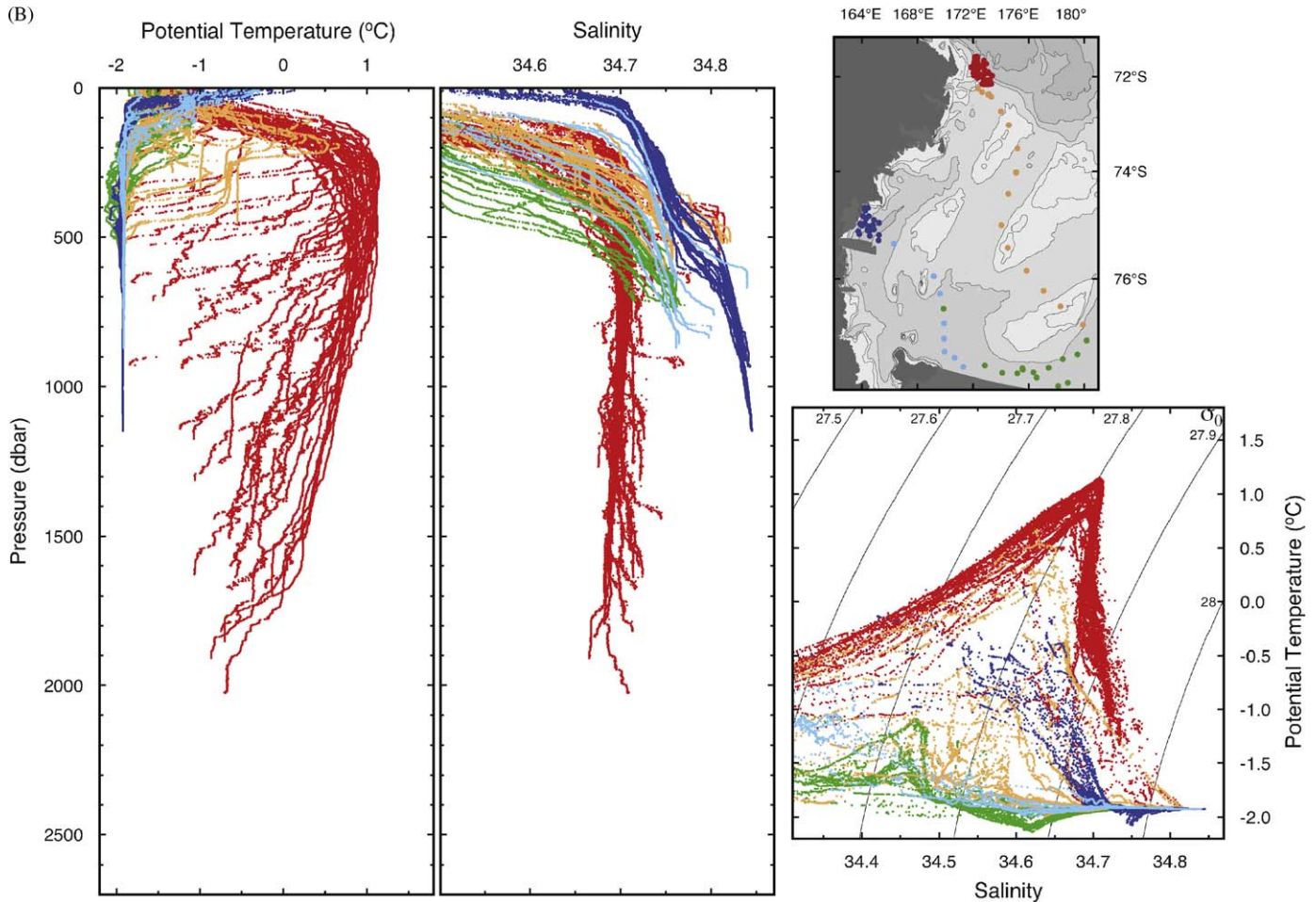


Fig. 2. (Continued)

water enters into the southeast Pacific Basin, as suggested by bottom-water flow patterns (Gordon, 1966; Orsi et al., 1999), rather than veering westward to parallel the slope around the northern flank of Iselin Bank. Along the western flank of Iselin Bank, and adjacent to the outlet of Joides Trough, bottom water was warmer and more saline ($0.2\text{ }^{\circ}\text{C}$, 34.68) than along the eastern flank of Iselin Bank.

A pronounced change occurs in 2003 near 177°E , west of which the bottom water becomes progressively colder and saltier ($-0.5\text{ }^{\circ}\text{C}$, 34.69). Continuing this trend west of 173°E , it becomes still more saline (>34.7). Based on access of HSSW (Fig. 4) to the continental slope, the pattern west of 177°E reflects an export through Joides Trough of cold, intermediate level saline water (upper stratum of the HSSW), with the addition of more saline deeper layers within the HSSW into the benthic layer adjacent to Drygalski Trough. Station to station fluctuations of bottom-water temperature and salinity likely reflect tides and the controlling influence of small-scale topography, both of which tend to obscure the regional representation. Bottom water adjacent to Drygalski Trough was slightly less saline in 2004 than in 2003 (Fig. 3).

The distribution of bottom-water temperature and salinity suggest a mean flow pattern (Fig. 1A, inset). In the east, relatively low-salinity Shelf Water is channeled to the continental slope by the Glomar Challenger Trough. Much of this water flows down-slope and subsequently spreads along the sea floor of the Southeast Pacific Basin (Gordon, 1966; Orsi et al., 1999), based

on the water properties at 1000–2000 m isobaths along the northern and western flanks of the Iselin Bank. Bottom-water properties indicate that some water curls around the Bank towards the west. Cooler bottom water is observed at the mouth of Joides Trough, with further cooling and significant salinity increase adjacent to Drygalski Trough. Some Joides Trough outflow may flow around the bank near 177°E before rejoining the general westward flow.

Westward salinity increase within the slope benthic layer (Figs. 2 and 3) reflects the regional distribution of shelf water masses (Fig. 4), as HSSW mass is shifted towards the western boundary (see Fig. 9 of Orsi and Wiederwohl, 2009). The 34.7 isohaline deepens eastward, from 150 m at the western boundary to where it intercepts the sea floor at ~ 500 m near 173°W . Bottom-water salinity in the westernmost trough, Drygalski Trough, is ~ 34.9 . The Terra Nova Bay Polynya (Bromwich and Kurtz, 1984), which is located over the deeper parts of the Drygalski Trough, has been shown to be a primary source of this highly saline HSSW (Budillon and Spezie, 2000).

Increased benthic-layer salinity over the western Ross Sea continental slope reflects the greater access of HSSW to that region. The most saline and the densest HSSW layers are trapped within the topographic depression formed by sills at the shelf break. The trapped components of HSSW water may flow poleward reaching below the Ross Ice Shelf before returning north as ISW, or alternately may mix upward to gain more immediate access to the open ocean. Comparison of the zonal

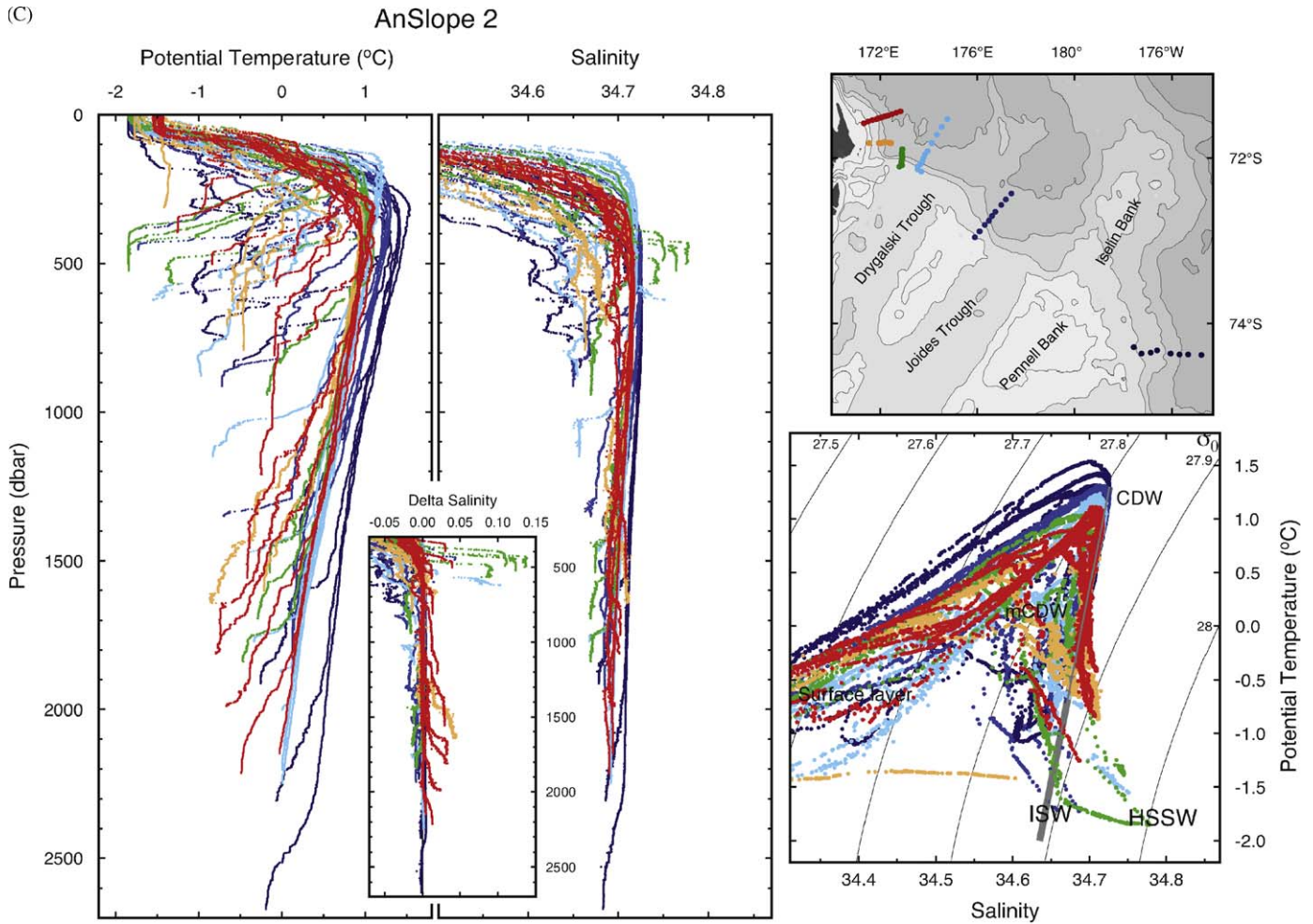


Fig. 2. (Continued)

salinity distribution to the sill depth at the Ross Sea outer shelf (Fig. 4) indicates that the 34.82 water, well within the HSSW volume, has access to the open ocean over the Drygalski Trough 510 m sill. Shelf Water with salinities of 34.78 has access through the Joides Trough 510 m sill. The Glomar Challenger Trough sill is the deepest of the three sills, about 570 m, yet because of the confinement of HSSW to greater depths than within the Drygalski Trough, the escape of HSSW to the open ocean via Glomar Challenger Trough is restricted to salinity of less than 34.72. The Glomar Challenger Trough however is richer in ISW characteristics than the more western troughs.

Jacobs et al. (2002) report a general freshening by 0.1, from the 1960s to 2000, of Ross Sea HSSW waters observed along the front of the Ross Ice Shelf. They attribute this to increased precipitation and accelerated glacial ice melting. If this salinity change extends throughout the HSSW volume, then it may be expected that bottom water over the continental slope would have been similarly reduced in volume over the same period. As always, analyses of observational “snap-shots” of ocean conditions need to be tempered in view of longer-term trends.

In addition to sill-controlled access, the descent of Shelf Water to the deep ocean may reflect aspects of the seawater equation of state. The θ/S distribution shown in Fig. 2 indicates that ISW (34.62 near the Ross Ice Shelf front) could serve as the cold end-member for an apparent two point mixing recipe with “pristine” CDW of the oceanic domain (Brennecke, 1921; Mosby, 1934) in the production of AABW. This recipe is thought to be active in the

Weddell Sea, with the role of CDW filled by Weddell Deep Water (WDW; e.g. Foldvik and Gammelsrød, 1988). However, ISW and CDW are not juxtaposed in the western Ross Sea, and a new volumetric census of Ross Sea water types indicates that ISW ($< -1.95^\circ\text{C}$) represents but a minor (7.5%) fraction of the available Shelf Water volume (Orsi and Wiederwohl, 2009). In contrast, large volumes of MCDW overlie HSSW ($< -1.85^\circ\text{C}$ and > 34.62) in the Ross Sea and are present throughout the central and western Ross Sea. Despite its small volume flux it is feasible that the ISW still plays central role in shaping the Ross Sea gravity-current thermohaline properties through the thermobaric “compressibility” effect (McDougall, 1987; McPhee, 2003), as mentioned in Section 3. In a mixture of MCDW, HSSW, and ISW, by virtue of the thermobaric effect, the coldest blend that most enriched in the ISW component, is most likely to sink to the deep ocean once it is exported across the shelf break. Because the bulk of ISW is found in the central Ross Sea, the thermobaric effect may be crucial to the less saline ISW generated within Terra Nova Bay Polynya serves as the cold end-member for the salty benthic layers of the western Ross Sea slope.

This multiple water type recipe is similar to that described for the Weddell Sea by Foster and Carmack (1976a, Fig. 12; Foster and

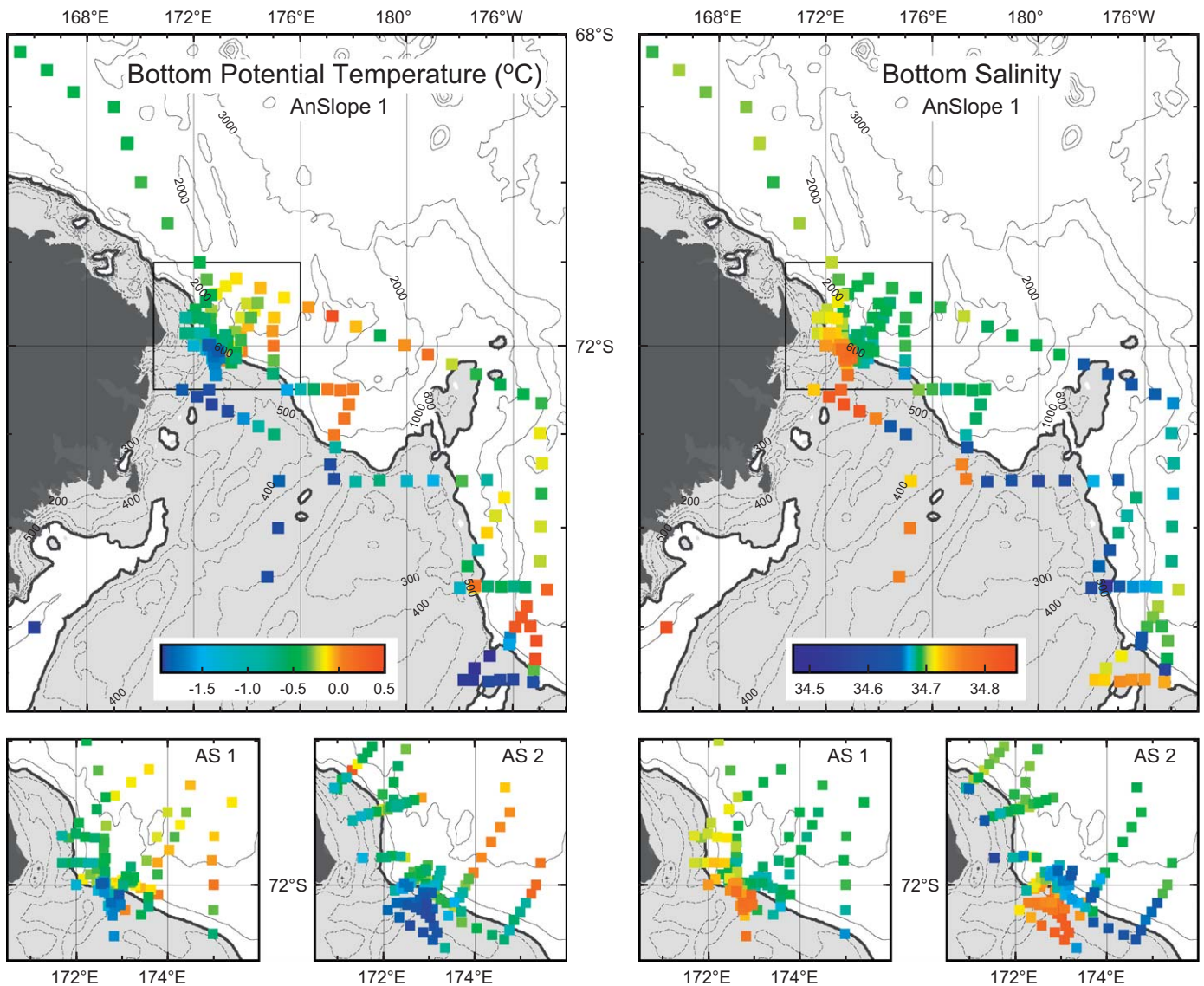


Fig. 3. Potential temperature and salinity of the lower 20 m of the water column. The 600 m marking the approximate position of the shelf/slope break isobath is shown by a thick black line. The upper panels show summer 2003 data, with potential temperature in the upper left and salinity in the upper right. The smaller insets, lower panels, show summer 2003 and 2004 bottom values adjacent to the Drygalski Trough, with potential temperature in the left pair of lower panels, salinity in the right pair.

Carmack, 1976b) in which they suggest that the WDW (0.5°C ; 34.68) mixes with Weddell Sea Bottom Water (-1.3°C , 34.64), which is a 50–50 mixture of Modified Weddell Deep Water (-0.8°C , 34.59) and Weddell Shelf Water (-1.9°C , 34.70). This was first suggested by Gill (1973) as an alternate recipe to an earlier AABW formation theory (Brennecke, 1921 and Mosby, 1934) that depended on a simple two-end-member blend of near-freezing shelf water at 34.62 and CDW.

5. Bottom-water flow off Cape Adare

Regional circulation associated with the Ross Sea continental slope upstream from Cape Adare is westward, as seen both in the moored observations and in instantaneous current measurements from LADCP observations coincident with CTD profiling during AnSlope cruises. Interpretation of current observations from the AnSlope moorings required allowance for the extreme spring tidal blowdown of the moorings and the accompanying degradation of data quality. Vertical excursions of any but the near-bottom

instruments, which were $\sim 10\text{ m}$ above the seafloor, were large and exceeded 100 m in many cases. These depth excursions preclude meaningful long-term averages at specified depths. Given the curvature anticipated for a mooring under lateral stress from strong currents, the near-bottom instruments were subject to tilting, which in extreme cases would have impacted the speed rotor response. Further, tilt-induced depth changes of only a few meters within the bottom frictional boundary layer would contribute to speed biases. To avoid these potential errors, means were constructed using data only from 3-day periods during neap tides when blowdown was negligible. The means are thus derived data that were burst-sampled over 3-day periods coinciding with those times when the current meters were not being impacted by depth fluctuations and possible tilting due to blowdown. Data from the intervening $\sim 11\text{-day}$ intervals were discarded.

This use of burst-sampling leads to means that we believe reasonably represents neap tide conditions. It is likely nonetheless that some enhancement occurs at other times through nonlinear interactions and perhaps also through the large cross-slope excursions. In fact, the computed means do not include the

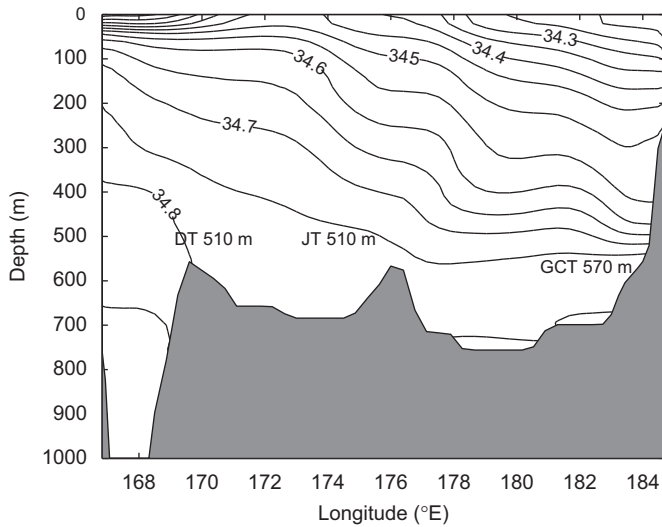


Fig. 4. Zonal salinity section constructed from archived salinity data within a narrow band transiting approximately the mid-shelf of the Ross Sea. Gray shading indicates the approximate bathymetry along the transit. The depths of sills separating the shelf from the deep ocean are given for the three primary north–south troughs: Drygalski Trough (DT), Joides Trough (JT), and Glomar Challenger Trough (GCT).

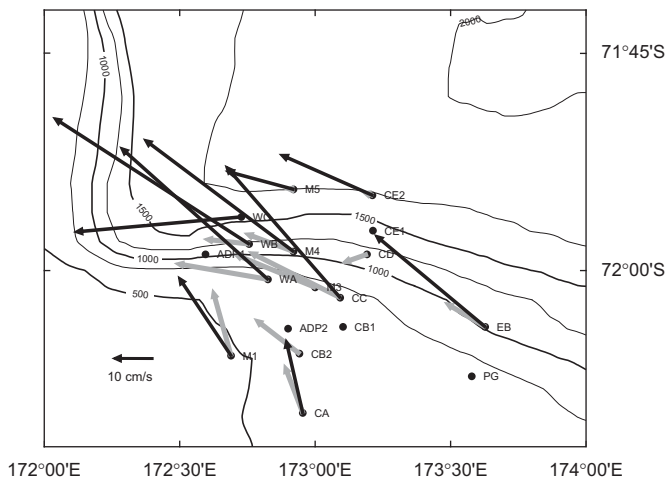


Fig. 5. Map of the AnSlope mooring locations (see Table 1). Vectors show the long-term mean currents at mid-water depths (gray; the values marked with + in Table 2) and at the sea floor (black; the values marked with * in Table 2) derived from the 3-day neap tide periods in order to minimize potential errors caused by extreme mooring blowdown by spring tidal currents. See text for further explanation.

episodic and strongly downslope flow events reported by Gordon et al. (2004), because these events were associated with spring tidal periods. Quantitative assessments of these effects falls outside the scope of this work and are planned to be addressed in model-based studies.

Given these caveats, mean westward slope current speeds were typically $0.1\text{--}0.2\text{ m s}^{-1}$, with the highest speeds near the upper slope, 700–800 m (Fig. 5 and Table 2). The bottom current is everywhere stronger than at mid-depths, with an increased downslope component as we would expect in the presence of gravity current. The flow pattern formed by the vectors is in qualitative agreement with the water-mass based pathways (Fig. 1A).

The regional slope circulation, upon reaching the western limits of the Ross Sea adjacent to the Victoria Land Coast, veers sharply northward to follow the bathymetry of the continental

Table 2
Record-length mean neap currents (cm s^{-1}).

Depth	Westward (+)		Northward (+)	
	Mean	Std	Mean	std
<i>CENT-A (505 m)</i>				
377 ⁺	4.7	4.5	12.2	4.8
484 [*]	4.3	3.6	18.7	6.2
<i>CENT-B2 (525 m)</i>				
381 ⁺	11.4	3.9	8.8	3.8
<i>CENT-C (651 m)</i>				
449 ⁺	23.4	6.3	11.7	3.4
551	33.6	7.5	10.8	3.6
630 [*]	29.5	4	33.8	4.1
<i>CENT-D (1118 m)</i>				
508 ⁺	6.2	5.1	−2.2	1.2
716	6.9	4.3	2.3	2
<i>CENT-E2 (1772 m)</i>				
461 ⁺	2.5	1.8	0.8	1.1
677	1.2	1.3	0.6	1
1751 [*]	23.7	6.1	10.4	3.4
<i>WEST-A (609 m)</i>				
419 ⁺	23.7	11.1	4	6
587 [*]	38	2	33.9	8.2
<i>WEST-B (1025 m)</i>				
432 ⁺	11.4	4.2	1.2	1.3
632	13.1	5.6	2.2	1.9
1004 [*]	50.4	3.3	32.4	7.7
<i>WEST-C (1630 m)</i>				
1238	12.6	4.8	8.5	5.3
1609 [*]	42.9	5.5	−4	4.9
<i>EAST-B (982 m)</i>				
586 ⁺	10.2	11.7	6.1	12.2
961 [*]	28.3	11.1	23.5	11.8
<i>M1 (498 m)</i>				
248	6.3	4.3	7.9	4
398 ⁺	4.7	3.9	16.8	4
478 [*]	13.5	2.9	20.2	5
<i>M3 (691 m)</i>				
391 ⁺	20.9	6.2	8.5	2.7
491	26.5	6.3	12.8	3.2
<i>M4 (984 m)</i>				
384 ⁺	12.4	3.9	4.6	1.7
784	36.4	4.8	6.6	2
964 [*]	38.5	3.7	28.8	7.6
<i>M5 (1749 m)</i>				
449 ⁺	1.9	2	0	0.8
1049	−0.5	2	0.5	0.9
1729 [*]	17.2	5.5	4.6	2.1

Mooring, water depth; * and + indicate bottom [black] and mid-water [gray] currents shown in Fig. 1B.

slope until it exits the Ross Sea near Cape Adare. Each AnSlope cruise occupied cross-slope station transects off Cape Adare. The stations from AnSlope-2 (Fig. 6A) provide the most detailed

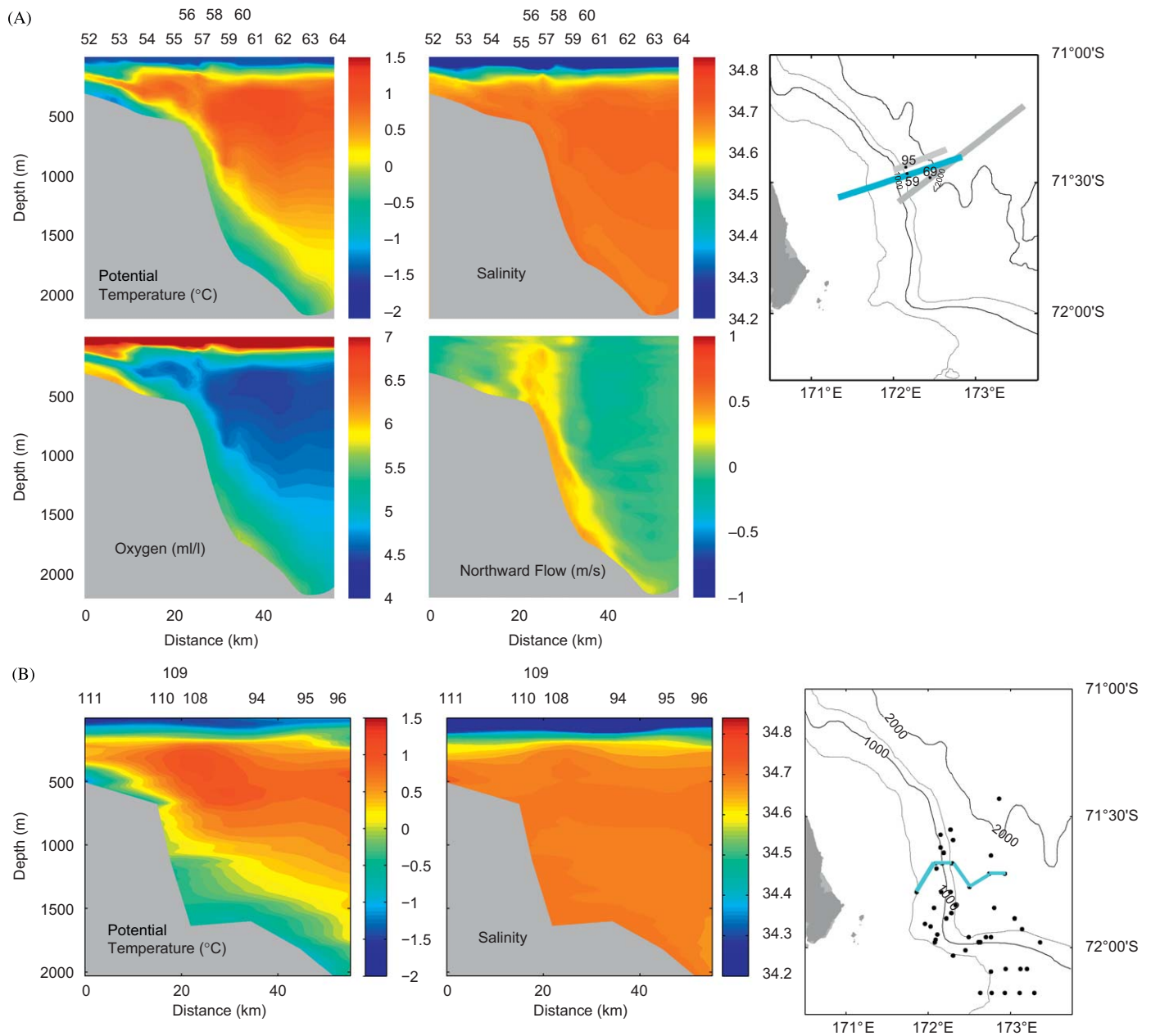


Fig. 6. (A) Summer 2004 section of potential temperature, salinity, oxygen and speed (+ is towards the north) adjacent to Cape Adare, section location shown in map inset. (B) Similar to (A), only for a January 2003 (CLIMA) section adjacent to Cape Adare.

picture. A distinct cold, highly oxygenated benthic northward-flowing layer is clear over the continental slope.

AnSlope-1, 2, and 3 Cape Adare profiles of θ , S , σ_1 (potential density anomaly referenced to 1000 dB) and LADCP-measured shear near 1500 m depth off Cape Adare (Fig. 7) reveal further details of the benthic layer. The vertical mean current (roughly, the barotropic portion, $\sim 0.1 \text{ m s}^{-1}$ directed northeast to northwest and assumed primarily tidal) of the water column has been removed to isolate the strong baroclinic signal within the benthic layer.

Bottom flow off Cape Adare parallels the southeast–northwest oriented local isobaths, at speeds in excess of 0.5 m s^{-1} , from the shelf break at 600 m to nearly 2000 m. Elevated salinities reflect the presence of HSSW water that is derived from Drygalski Trough, though contribution of lower-salinity bottom water derived from Joides Trough, or westward flow from farther east

over the northern edge of Iselin Bank, is also likely (Gordon et al., 2004). While the cold, saline bottom water is observed throughout the region of speed $> 0.5 \text{ m s}^{-1}$, the coldest and most oxygen-rich bottom water is found in the 1500–1800 m range (Fig. 6A). Assuming this is mainly derived from the Drygalski Trough by export of HSSW across the shelf break 600 m isobath, the 1000 m descent over a slope of roughly 1:10 [the slope between 600 and 1600 m off Cape Adare is 1:10; see Fig. 6A; adjacent to Drygalski Trough the slope is slightly steeper, 1:8] in a distance of about 45 km, requires a mean descent angle to the local isobaths of 12.5° , but this is mostly accomplished within the first 2 km of the distance to Cape Adare by a rapid ($\sim 40^\circ$ to the local isobath) descent to ~ 1000 m over the upper slope near Drygalski Trough (see Fig. 1B, Gordon et al., 2004). This is followed by more of an isobath-following flow over the remaining path to Cape Adare.

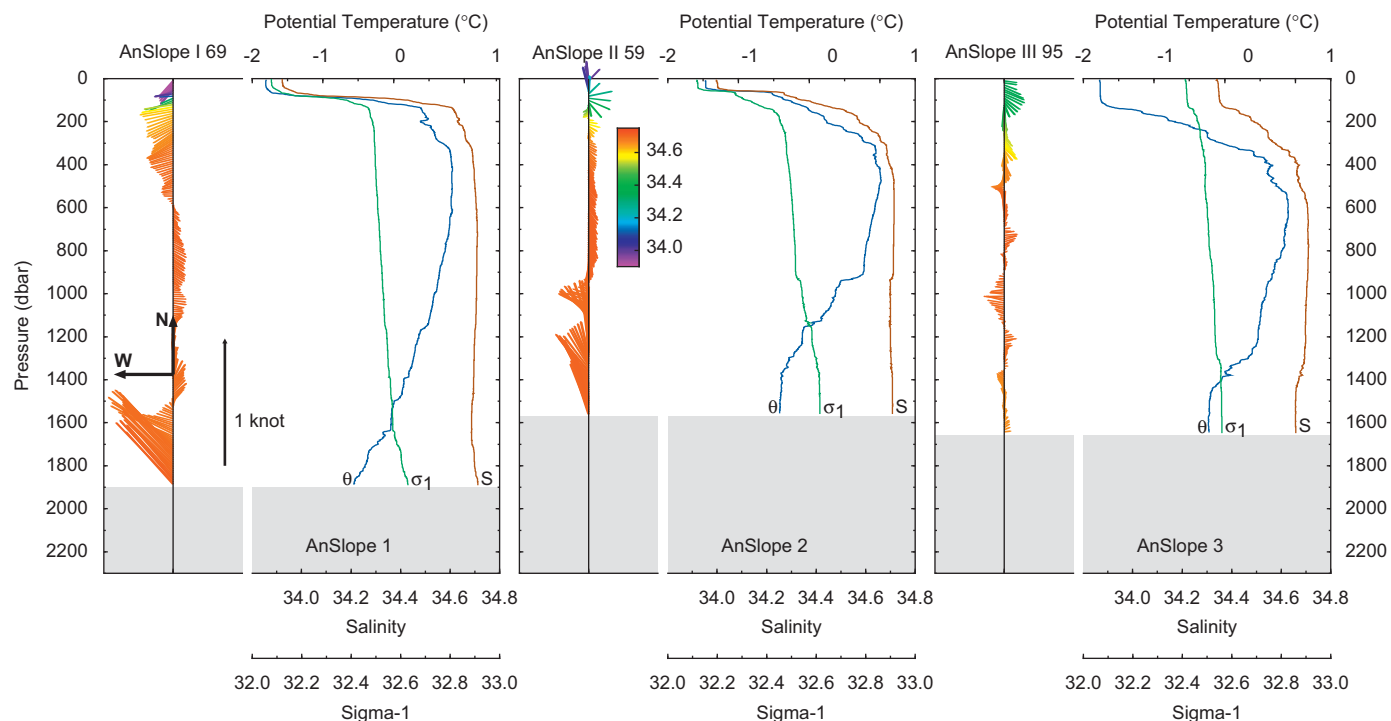


Fig. 7. Profiles from summer 2003 and 2004 and winter 2004 of potential temperature (θ), salinity (S) and sigma-1 (σ_1 ; density anomaly at a pressure of 1000 dbar), and baroclinic currents (north is pointed upward along the base line). The mean (barotropic, mostly tidal) water-column current has been removed to better show the benthic layer.

The January 2003 CLIMA CTD section (Fig. 6B) further documents the stratification off Cape Adare. The decrease of potential temperature and increase of salinity as the sea floor is approached is clearly defined in the θ/S scatter (inset of Fig. 2B). Extension to the freezing point of the linear fit to the benthic θ/S slope shows a cold end-member at ~ 34.75 . The AnSlope-1 and AnSlope-2 stations off Cape Adare indicate the same cold end-member (Fig. 2A and C). While the cold end-member is clearly within the HSSW θ/S range, it is more specifically within that characterized by the Terra Nova Bay ISW (Fig. 2B), further suggesting a central role of ISW in determining the AABW characteristics as discussed above.

Benthic-layer thickness over the continental slope off Cape Adare, as determined from the overlying strong density gradient, was 300–400 m (Fig. 7). The benthic layer exhibited speeds, based on instantaneous summer 2003 and 2004 measurements, of $\sim 0.5 \text{ m s}^{-1}$, directed towards the northwest roughly along the isobaths. During early spring 2004 (AnSlope 3), benthic-layer salinity was lower than that of the overlying water whereas both AnSlope-1 and -2 showed increased salinity in the benthic layer. This is consistent with the scalar time series from the AnSlope moorings, discussed below, which show much reduced HSSW export during austral winter and spring as compared with summer. In addition, the bottom intensified baroclinic layer was absent from the AnSlope 3 data.

The transport of benthic-layer water along the slope between the 1000 to 2000 m isobaths (cross-slope distance of 18 km) past Cape Adare is estimated from the 13 AnSlope-2 CTD/LADCP stations. The benthic-layer flow was directed north-northwest, aligned approximately along isobaths, with an average speed of 0.3 m s^{-1} (sum of the baroclinic and barotropic, the latter rarely above 0.1 m s^{-1}), within the $\sim 300 \text{ m}$ thick benthic layer. The resulting estimated transport is 1.7 Sv. From the linear fit in θ/S space of the benthic-layer spanning the θ/S distance from the lower CDW to the HSSW, we estimate that HSSW composes 25% ($\sim 0.4 \text{ Sv}$) of this transport. None of the four winter 2004

(AnSlope 3) stations off Cape Adare showed bottom intensification characteristic of the dense benthic current. If the export of Drygalski Trough outflow is a 6-month duration (summer/fall) event, consistent with the AnSlope mooring time series discussed below, then an annual average transport of benthic-layer water is 0.8 Sv with 0.2 Sv consisting of HSSW.

HSSW is lost at its southern limits through conversion to ISW under the Ross Ice Shelf, as well as northward through direct export to the open ocean over the shelf break and slope. Smethie and Jacobs (2005) used CFC data to determine a production rate of ISW water of 0.86 Sv through conversion of HSSW. Assuming no export east of Drygalski Trough of HSSW containing significant ISW, then the total export of HSSW is 0.2 Sv plus the 0.86 Sv of ISW flux (Smethie and Jacobs, 2005) or $\sim 1.0 \text{ Sv}$. Using a HSSW volume for the Ross Sea of $1.29 \times 10^{14} \text{ m}^3$ (Jacobs et al., 1970) yields a HSSW residence time of 3.8 years. Using the smaller HSSW volume of $0.716 \times 10^{14} \text{ m}^3$ estimated by Orsi and Wiederwohl (2009) yields a HSSW residence time of 2.1 years. The 2- to 4-year HSSW residence time should be considered an upper bound, as there is likely some direct export of HSSW from Glomar Challenger Trough that might not pass by Cape Adare, but rather flows directly into the Southeast Pacific Basin. Of course, as is often the situation in observational oceanography, there is no reason to expect that the AnSlope 2003–2004 period represents a “typical” period.

6. Western Ross Sea gravity current characteristics

The continental slope benthic-layer thermohaline and current characteristics observed in summer 2003 are briefly described by Gordon et al. (2004). Here, we update this discussion using summer 2004 CTD/LADCP observations.

The baroclinic bottom speeds (lower 20 m, Fig. 8) are based on instantaneous rather than long-term time-series measurements; however, there are sufficient instantaneous observations, that are

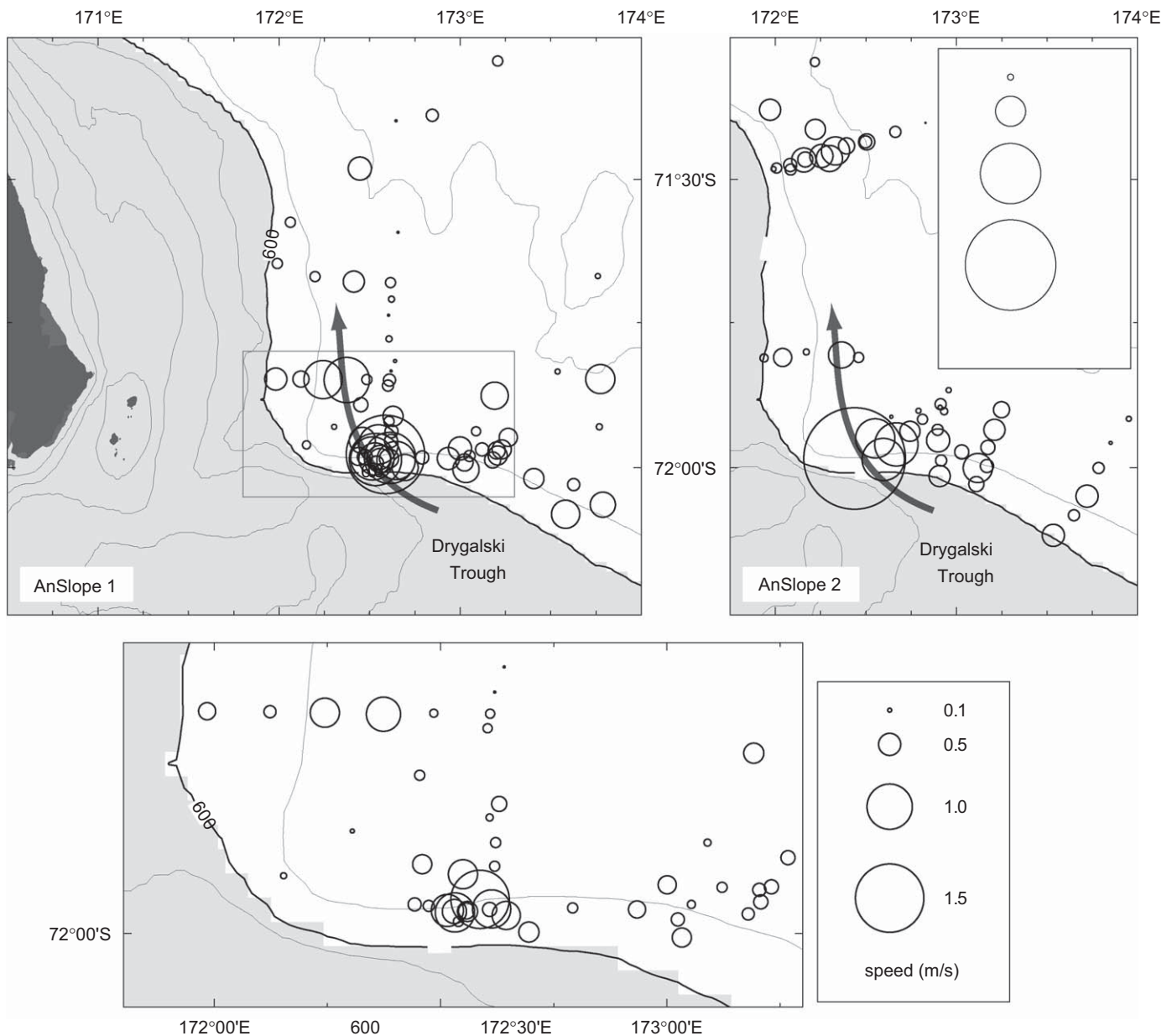


Fig. 8. LADCP-derived scalar speeds within the lower 20 m for summer 2003 (left panel) and 2004 (right panel). The mean (barotropic) water-column current is removed to better display the gravity current. The arrow shows the path followed by the outflow of saline water from the Drygalski Trough. An expanded map is shown for the cluster of 2003 stations in the vicinity of the AnSlope moorings (see Fig. 5).

consistent with the temporal mean “neap” bottom vector (Fig. 5) to “reasonably constrain” the regional distribution of bottom speeds. The regional average benthic-layer speed over the slope of the western Ross Sea was 0.4 m s^{-1} , whereas within Drygalski plume benthic speeds in excess of 0.7 m s^{-1} were common, often approaching 1.0 m s^{-1} . Gordon et al. (2004) using the 2003 CTD/LADCP data show that the more saline and denser benthic layer was associated with higher speeds and, further, that it descended downslope on average at 40° to the isobaths over the upper slope ($< \sim 1500 \text{ m}$). Deeper than $\sim 1500 \text{ m}$, the benthic flow turned westward to closely parallel the general isobath trend. However, direction and speed of the bottom current varied with episodic downslope cascades, close to 90° to the isobaths (Gordon et al., 2004). The large variability makes it difficult, or perhaps unrealistic, to draw a regional picture other than to note the general differences of the energetic gravity current adjacent to

Drygalski Trough relative to the reduced speeds of 0.4 m s^{-1} over the eastern flank of Iselin Bank and below 0.1 m s^{-1} over the western flank of Iselin Bank.

The pathway of the energetic, saline outflow from Drygalski Trough can be traced using CTD/LADCP stations from summer 2003 and 2004 (Fig. 9A). The summer 2003 benthic layer was slightly more saline than that observed in summer 2004, though no significant change was apparent in vertical shear. The barotropic current (removed from the profiles) was strongest over the outer shelf and upper slope reflected strong local tidal currents (Erofeeva et al., 2005; Padman et al., 2009). At 1200 m , the barotropic current varied from $\sim 0.1 \text{ m s}^{-1}$ at station 37 to $\sim 0.4 \text{ m s}^{-1}$ at station 83. For the two stations along the north-south trending 1700 m isobath, barotropic flow was $0.1\text{--}0.2 \text{ m s}^{-1}$. The direction of the barotropic current (LADCP) shows no pattern that can reasonably be associated with the regional scale

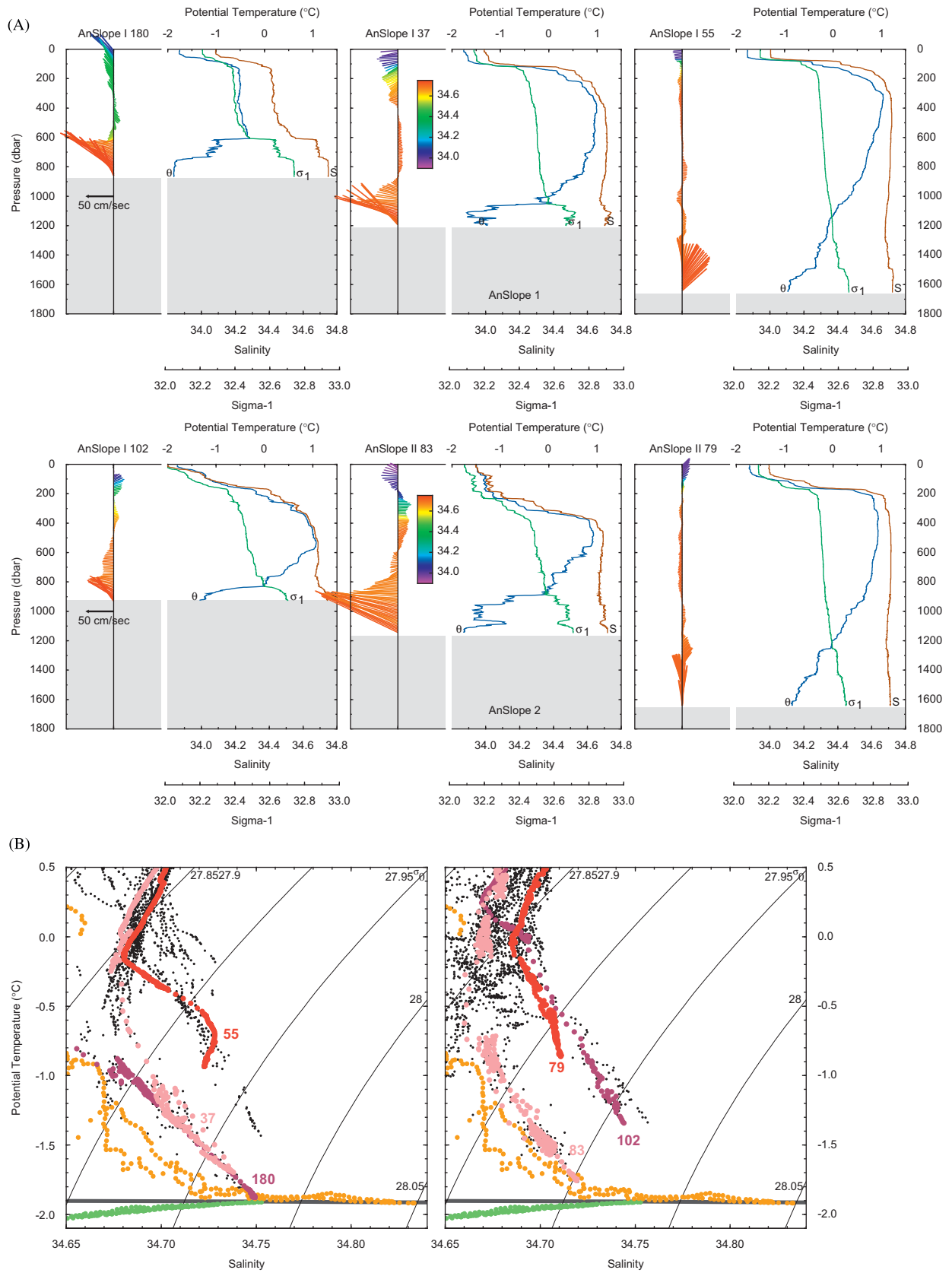


Fig. 9. (A) Potential temperature, salinity and σ_1 profiles of three CTD/LADCP stations from summer 2003 (upper panels) and three CTD/LADCP stations from summer 2004 (lower panels) that are situated along the path of high-salinity bottom water derived from Drygalski Trough (arrow on Fig. 7). Velocity profiles (mean current removed) from LADCP every 10 dB are color coded for salinity. Distances between the AnSlope-1 and -2 stations are as follows: 180-102: 2.1 km; 83-37: 5.2 km; 55-79: 4.8 km. (B) The θ/S scatter of all summer 2003 and 2004 data west of 174°E between the 700 and 1500 m isobaths (black). Also shown are the Drygalski Trough HSSW (orange line) and the lower-salinity type from the Glomar Challenger Trough (green line). The θ/S scatter for stations in (A) are shown in color (for interpretation of the references to color in this figure legend, the reader is referred to the web version of this article).

circulation of the Ross Gyre, again attesting to the tidal origin of the barotropic flow coupled with sampling during difference phases of the tidal cycle.

The internal Froude number, Fr , a dimensionless number of the ratio of inertial to static stability, is used to determine if a flow is supercritical (turbulent, $Fr > 1$) or subcritical (laminar, $Fr < 1$). For gravity flows, $Fr = U/(g'H)^{0.5}$, where U is the difference in speed as determined by the LADCP profile across the upper boundary of the gravity current, g' the reduced gravity, and H the thickness of the gravity current. Thickness H is estimated from the CTD/LADCP profiles by defining the “top” of the benthic layer as the depth where the σ_1 density deviates by more than 0.01 from a reference function $\sigma_1(p)$, which is taken as a linear fit to the $\sigma_1(p)$ of the

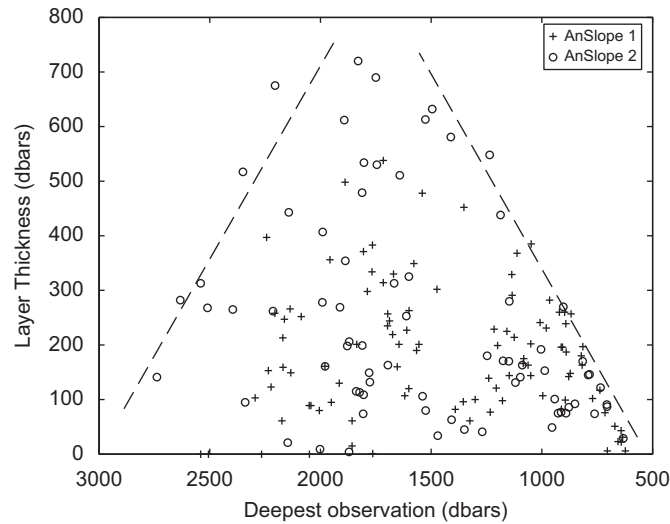


Fig. 10. Thickness of the benthic layer, H (m), for AnSlope-1 (+) and -2 (o) stations deeper than 600 m plotted against the sea floor depth.

deep water below the depth of θ_{max} . Values for stations shown in Fig. 9A range from 0.9 (station 37) to 1.6 (station 180), straddling the division between subcritical and supercritical flows and implying significant entrainment with the ambient water (see also Muench et al., 2008). The same is true for the summer 2004 stations shown in Fig. 9A (lower panel): 0.6 (station 102) to 1.4 (station 79).

The θ/S scatter (Fig. 9B) indicates a freezing point end-member within the HSSW: salinity of 34.77 in summer 2003, but with a range from 34.74 to 34.78 in summer 2004. The lower-salinity value observed in 2004 implies additional input from Terra Nova Bay ISW.

The thickness of the benthic layer (H , determined as described above) is plotted against bottom depth in Fig. 10. While there is considerable scatter, the maximum H values reveal a steady increase as bottom depths increase from 600 to 1200 m, with a peak H thickness of 400–500 m between the 1200 and the 1900 m isobath, followed by a drop-off to near zero at 2600 m depth. H values as high as 700 m were found north of Cape Adare, but these thick benthic layers were poorly defined and may reflect local mixing rather than gravity current dynamics. The shape of H versus sea floor depth (distance down the slope) would be consistent with an entrainment phase in which the thickness increases upon descent to ~ 1200 m, followed by a detrainment phase for depths deeper than ~ 1900 m. The unusually steep angle on the upper slope of the gravity current relative to local isobaths, where reduced gravity of the benthic layer is greatest, is taken to indicate the entrainment phase.

The thickest layers (Fig. 11) were found along the western Ross margin, where HSSW export via Drygalski Trough rapidly descends to the 1500 m isobath. East of Drygalski Trough the benthic-layer speeds were lower and thicknesses less. The highest bottom salinity, corresponding to the densest benthic layer, was associated with the strongest bottom current. For example, only when salinity was greater than 34.68 did gravity-current speed exceed $\sim 0.75 \text{ m s}^{-1}$ (this point is consistent with the time-series

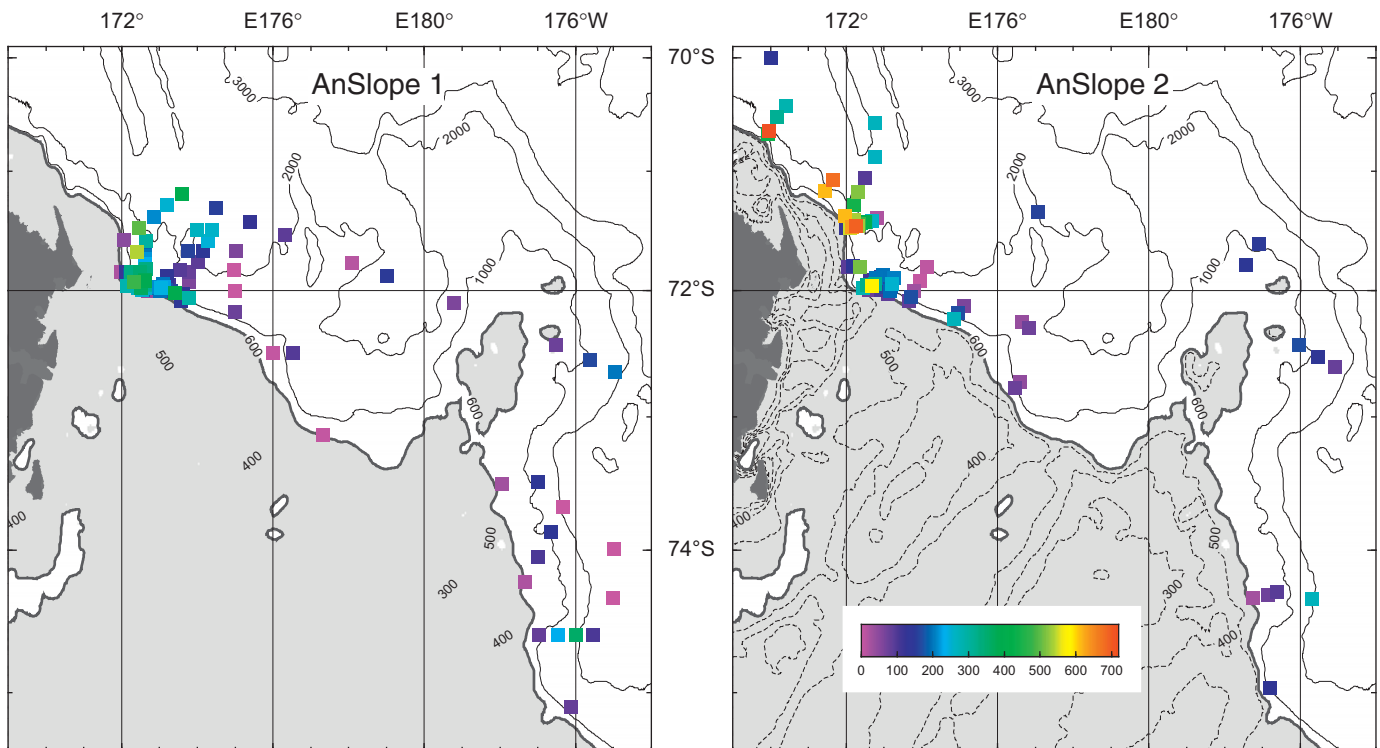


Fig. 11. Horizontal distribution of benthic layer thickness H (m).

data, discussed in the next section). Such episodes occurred when H was at its lower range, 150–350 m, typically occurring over the upper slope (<1000 m) during the initial descent phase of the shelf water.

7. Bottom-water time series

The mooring time series spanning the summer 2003–2004 periods connects the instantaneous observations of conditions during each of the two summers, allowing for at least a qualitative assessment of benthic-layer seasonal variability (Fig. 12).

The 30-day low-pass-filtered time series of near-bottom θ and S at selected sites on the shelf and slope reveal a clear seasonal signal (Fig. 12 lower panel). In austral winter (June–November 2003) near-bottom S at the seaward end of Drygalski Trough tracked by mooring CA (Fig. 5) was less than 34.74, and as low as 34.72 in the August and September period, ~0.05 fresher than observed earlier in April and May. Near-bottom S from November 2003 to February 2004 did not attain the high values measured in March–May 2003, being only 0.03 above the lowest winter values. Near-bottom salinity at CB2, located offshore of CA, was similar to the CA time series, though with 0.04–0.06 lower salinity (as expected from its position relative to the main mass of HSSW

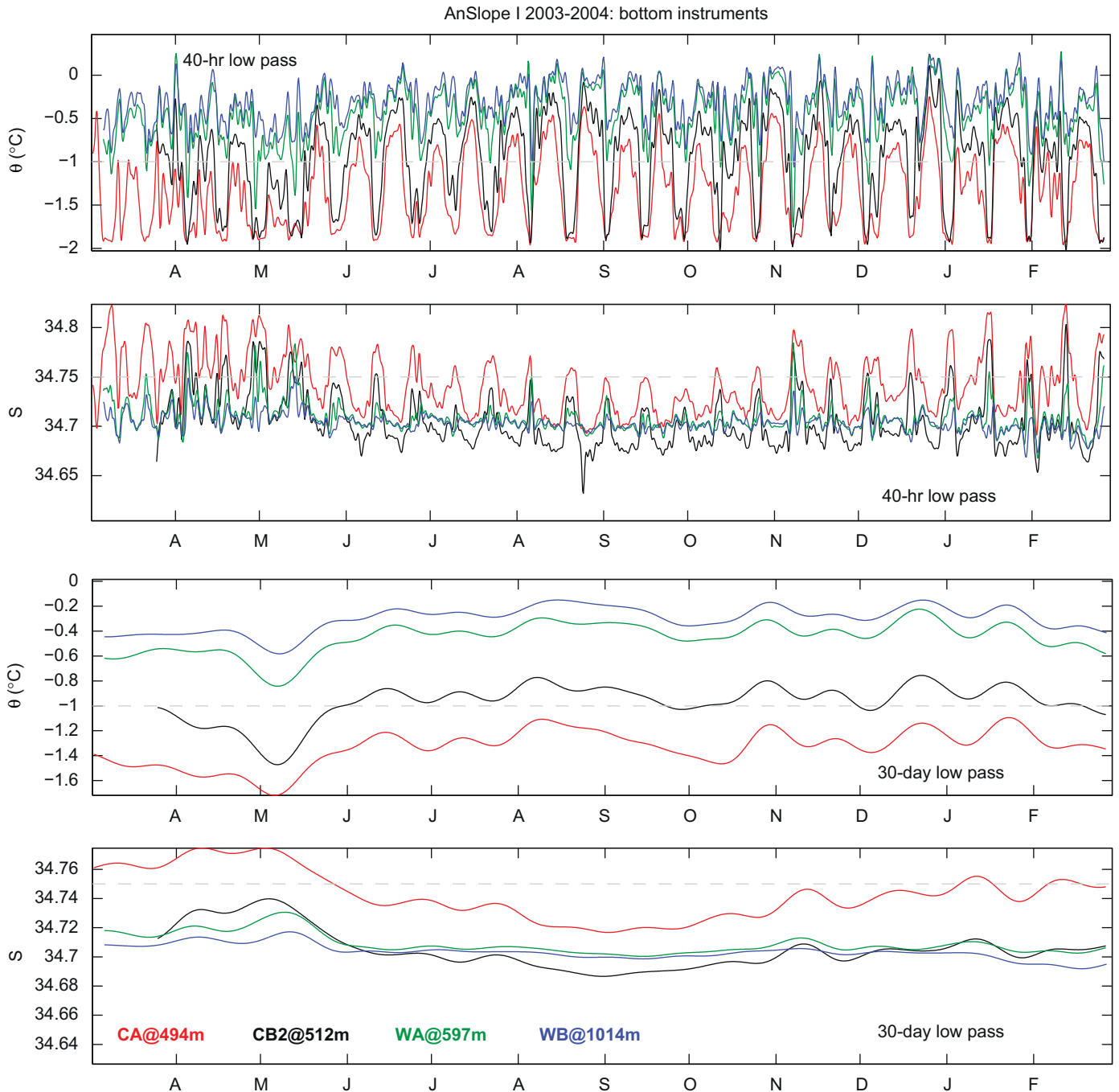


Fig. 12. Bottom potential temperature (θ °C) and salinity (S) time series from select AnSlope moorings (see Fig. 5 and Table 1 for mooring positions). The time series have been low-pass filtered at 40 h (upper panel) and at 30 days (lower panel). All data were collected using SeaBird MicroCats deployed within 15 m of the ocean floor, over a range of water depths ranging from inshore of the shelf break (494 m) to the lower slope (1761 m). Colored legends are placed according to the instruments geographical distribution (for interpretation of the references to color in this figure legend, the reader is referred to the web version of this article).

to the south). The associated bottom-water temperature at CA is as cold as -1.6°C in the March–May 2003 period, then oscillates about -1.3°C for the rest of the measurement period. A similar pattern of bottom temperatures is seen at CB2, though about $0.4\text{--}0.5^{\circ}\text{C}$ warmer. The CA and CB2 behavior is consistent with an attenuated flow of HSSW to the outer shelf after May 2003, with a partial recovery of flow strength after November 2003.

The near-bottom water close to the 600 m isobath, marking the shelf/slope transition, was sampled by the WA mooring. There, too, the near-bottom water was relatively salty and cold through May 2003. While S was slightly lower in the winter months, values achieved from November to February 2004 did not attain the levels seen from March to May 2003. WB, record of the

bottom-water behavior over the slope adjacent to Drygalski Trough, follows the trend of WA.

The 40-h low-pass time series (Fig. 12 upper) naturally reveals more of the full range of $\theta^{\circ}\text{C}$ and S values, as well as the energetic higher-frequency behavior shown by the tidal fortnightly (13.95 days, induced primarily by diurnal O1/K1 tidal components) oscillation, than does the 30-day low-pass time series. Ocean current variability translates to temperature and salinity variability only if there are substantial regional gradients of temperature and salinity such as occur in association with a front. The high-frequency oscillations in the bottom-water salinity and temperature were particularly pronounced in April–May 2003 when the coldest/saltiest bottom water was observed over the

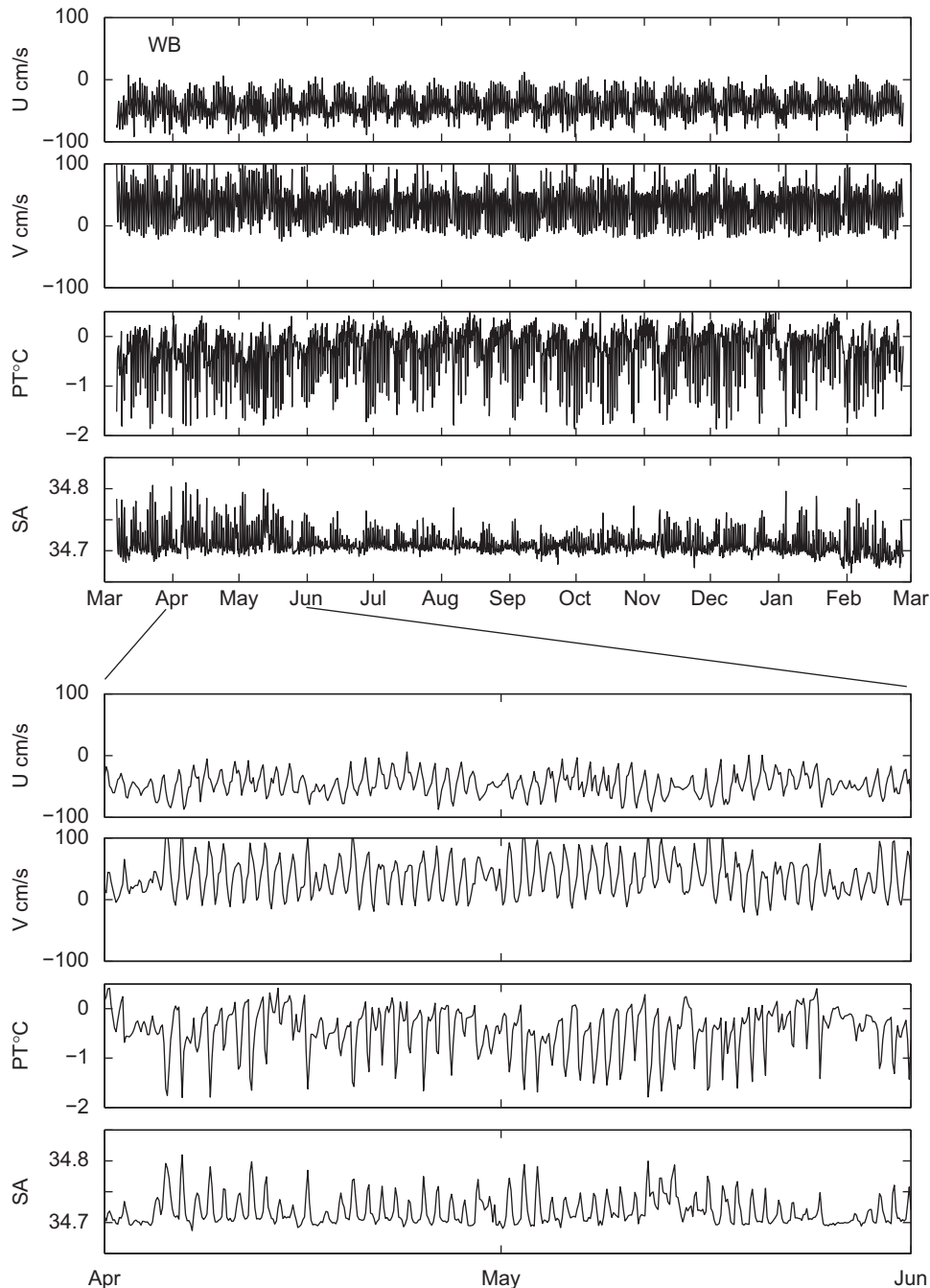


Fig. 13. The March 2003–March 2004 mooring WB time series at 1014 m (10 m above the sea floor) of zonal flow (u), meridional flow (v), potential temperature $\theta^{\circ}\text{C}$ and salinity (SA). The particularly variable period of April–May 2003 is shown in expanded form in the lower panel. Note the caveats in the text concerning reliability of moored current measurements during spring tides.

outer shelf and adjacent slope. The fortnightly oscillations had lower amplitudes from June to November 2003 than at other times. They increased in magnitude after November 2003, but never attained the high values present earlier in 2003. After May 2003, the mean salinity, as seen in the 30-day low-pass record, remains below the March–May 2003 peak levels. Bottom-water temperature fortnightly oscillations remained robust throughout the observational period. When the near-freezing water is salty, it is naturally denser and so forms a more energetic gravity current. The reduced salinity of the near-freezing point water in winter might reflect depletion of the saltier components of HSSW, a southward shift of the Antarctic Slope Front, or some combination of the two.

Bottom temperature and salinity time series (40 h low pass) at all moorings are visually well correlated (Fig. 12 upper panel). High-salinity bottom water ($S > 34.75$ and $\theta < -1.4$ °C) is exported during spring tides at shelf mooring CA (Muench et al., 2008), though between March and May 2003 the export of shelf water as salty as 34.75 also occurs during neap tides. Directly downstream, all spring tides at outer shelf mooring CB2 show temperatures below -1.2 °C and colder than -0.8 and -0.4 °C at WA and WB, respectively, on the upper slope.

Shorter period detail of the bottom-water temperature and salinity time series (30 min data points) and of bottom-water current over the continental slope at 1014 m as measured by mooring WB (keeping in mind the above caveat concerning contamination of current speeds during spring tide) is shown in Fig. 13. The record is punctuated with pulses of cold (< -1 °C), salty (> 34.75) events that correlate with strong northward flow. As suggested by the CTD/LADCP profiles, the salty gravity-current events flow directly downslope and faster than less saline events. Event timing was consistent with the fortnightly tidal cycle. The percentage of HSSW at ~ 1014 m at WB at times reached $\sim 100\%$ (-1.9 °C; 34.79), suggesting rapid descent from the outer shelf to the 1000 m isobath and negligible mixing with ambient slope water. The “down-hill” component more frequently exceeded 0.6 m s^{-1} before the end of May 2003 than later in the record, consistent with a greater export of HSSW in that period.

Though cold events with elevated northward bottom flow did occur occasionally during the winter months, notably the < -1.5 °C events of late June, September, and October, these rarely exceeded a salinity of 34.75, and so represent gravity currents presumably drawn from the upper layers of HSSW (Fig. 4), or possibly preconditioned by enhanced mixing.

While cold salty (≤ 1.0 °C and ≥ 34.75) benthic-layer events were detected during the entire record length, they were more commonly observed (87% of all cold/salty event observations) from March to 21 May 2003, and then again from 6 November 2003 to the record end in early March 2004, which together represent 54% of the total record length (Fig. 14). More specifically: 53% of these cold, salty events were observed from March to 21 May 2003 (21% of the time-series length) with 34% of the cold, salty events observed from November 2003 to March 2004 (33% of the record); during June–October 2003 (45% of the full record length) the observed cold, salty events contributed only 13% of the total observed events.

At mooring EB, 30 km east of WB, few if any HSSW outbreaks were observed (Fig. 15), in contrast to mooring WB, suggesting that the Drygalski plume turns westward during descent over the upper slope and misses the EB position. The EB site instead experienced lower-salinity bottom water derived from Joides Trough and possibly from Glomar Challenger Trough. The slightly lower temperature and salinity observed at EB from March to May 2003 and from December 2003 to March 2004 suggest a seasonal source for the export of low-salinity eastern Shelf Water, similar to

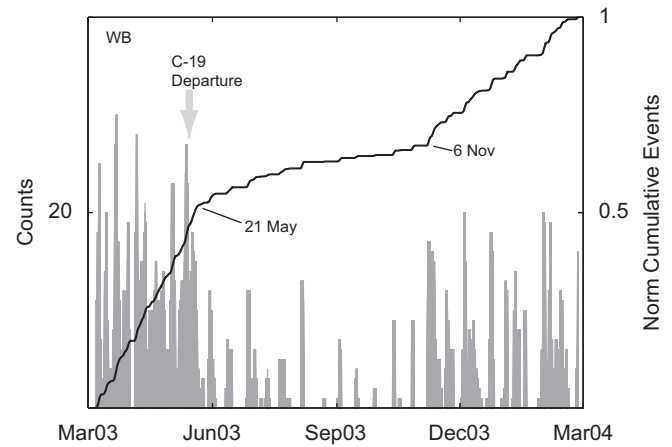


Fig. 14. The number of events (gray histogram; scale along the left axis) observed at mooring WB (see Fig. 5 and Table 1) at or colder than, -1 °C with a salinity at or greater than, 34.75 within a 48-h period. An event represents a 30-min sample. The cumulative events line from 0 to 1 is shown (scale along the right axis). From 13 to 25 May 2003, iceberg C-19 drifted north of and close to the AnSlope array.

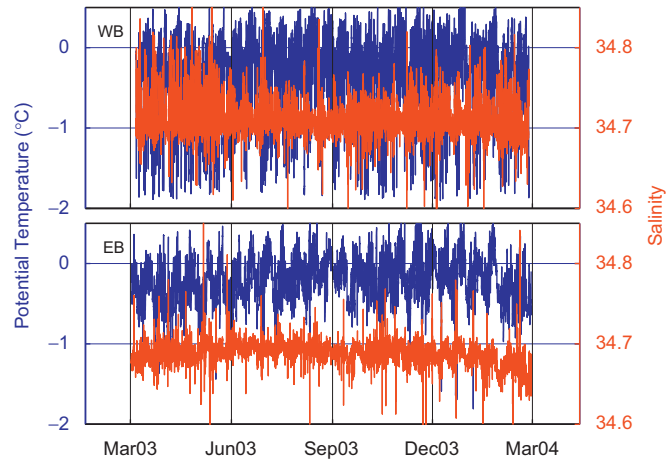


Fig. 15. Time series of near-bottom θ and S from mooring WB (1014 m), west of Drygalski Trough and EB (971 m), east of Drygalski Trough. EB is 30 km east of WB (Fig. 5 and Table 1).

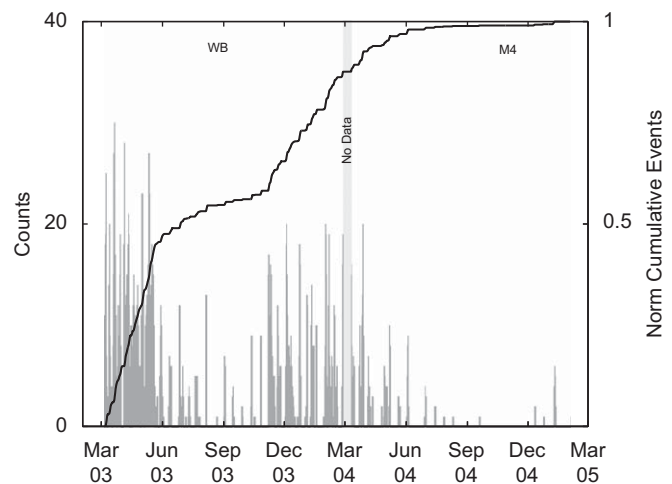


Fig. 16. The number of events at or colder than, -1 °C, with a salinity at or greater than 34.75, within sequential 48-h intervals over a 2-year period constructed by combining moorings WB and M4. M4 is ~ 6 km to the east of WB (Fig. 5 and Table 1). Display description as for Fig. 13.

the seasonality in export of the relatively salty Drygalski Trough shelf water.

A histogram of cold salty events over a 2-year time series was constructed by combining WB (2003–2004) and M4 (2004–2005), which was situated ~ 6 km to the east of WB (Fig. 16). In 2004, there was a dramatic reduction in such events after around 1 June, suggesting a seasonal signal similar to that seen in 2003. However, there were far fewer cold, salty events in summer 2004–2005 than in 2003–2004, which may reflect interannual variability in

the generation and export of HSSW. As a caveat, however, even the small (~ 6 km) separation between WB and M4 may be sufficient to respond to the geographical distribution of the plume path, given the local Rossby radius of ~ 5 km, favoring the more western position of WB.

The θ/S points, color-coded for speed (3-h running average) as observed at WB and M4 (Fig. 17), clearly reveal the relationship of gravity-current speed to its salinity and density. The θ/S scatter encompasses the mixing range of bottom water from the modified

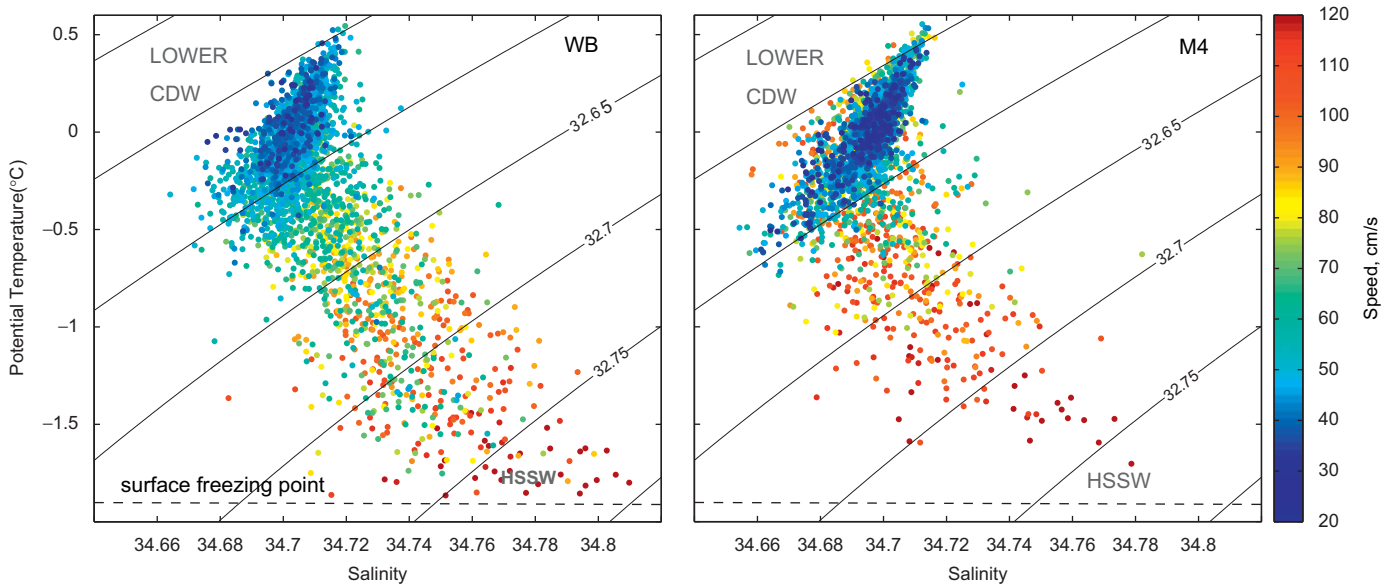


Fig. 17. Potential temperature/salinity scatter (θ/S) recorded at moorings WB and M4 near the sea floor and color-coded for speed. The data have been smoothed with a 3-h running average and subsampled at 3 h intervals (for interpretation of the references to color in this figure legend, the reader is referred to the web version of this article).

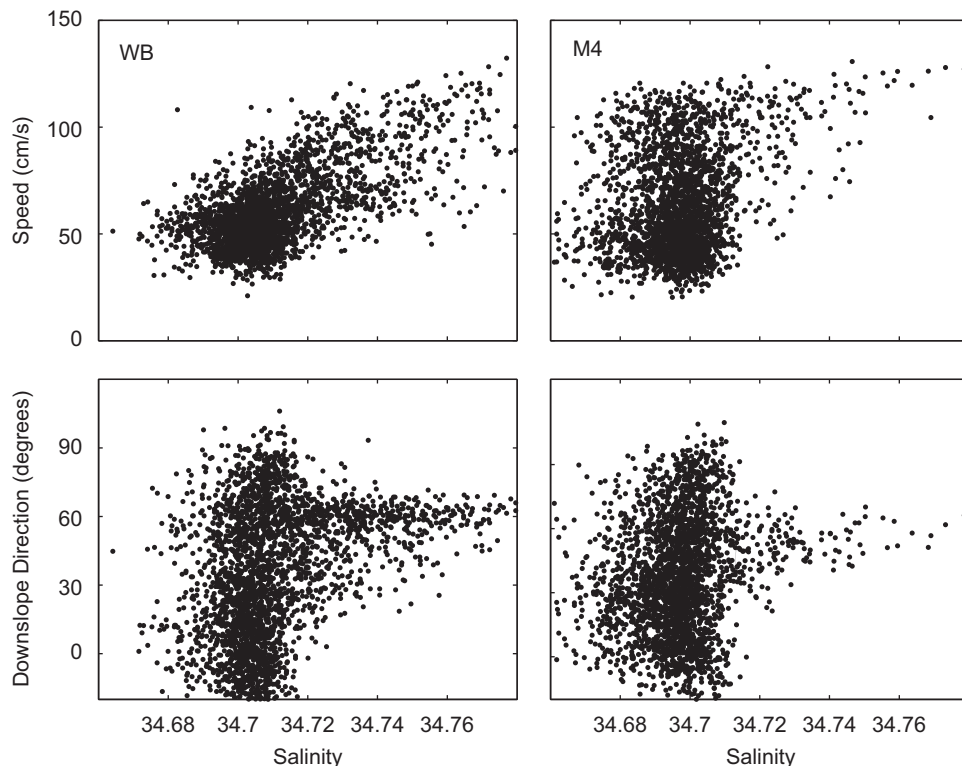


Fig. 18. Speed (cm/s; upper panels) and downslope direction (degrees of rotation from the regional isobath trend; lower panels) observed near 1000 m at moorings WB (left panels) and M4 (right panels). The data have been smoothed with a 3-h running average and subsampled at 3 h intervals.

CDW to nearly pure HSSW. Bottom currents of $\sim 1.35 \text{ m s}^{-1}$ observed by WB are associated with the saltiest of bottom-water events. M4 had fewer salty events. Approximately, 50:50 mixtures of modified CDW and HSSW had speeds of 0.75 m s^{-1} . The bottom speeds of the modified CDW θ/S were less than 0.4 m s^{-1} in WB, but were over 1.0 m s^{-1} in M4.

The relationship among bottom salinity, current speed and downslope angle is further explored in Fig. 18. The cluster of speed versus salinity is near 0.5 m s^{-1} and 34.7, with downslope angles of $0\text{--}90^\circ$ reflecting the combination of dense overflow, mean and tidal currents (see Padman et al., 2009). The WB (2003) time series shows greater frequency of HSSW outflow events than the 2004 M4 time series (also see Fig. 17). At WB, the increase of speed with increasing salinity is apparent, in excess of 1.3 m s^{-1} for a bottom salinity of 34.78, approximately pure HSSW. As salinity and speed increase the descent angle rotates towards 60° , presumably as the more energetic and topographically controlled gravity current become the more dominant signal. Though there are some energetic (up to $\sim 1.3 \text{ m s}^{-1}$) but less saline events (generally < 34.75) flowing at 60° downslope, they are less frequent than the more saline events. M4 recorded more high-speed events (~ 0.7 to 1.2 m s^{-1}) at lower salinity (~ 34.7), which the θ/S scatter (Fig. 17) identifies mostly as out flowing modified CDW, though some low-salinity Shelf Water was also present as indicated by $\theta \sim -1.0^\circ\text{C}$ and $S \sim 34.7$. The failure of WB to record rapid flow of modified CDW may reflect shortcomings in the mooring design, as pressure measurements from the shallower instruments on this mooring indicate extreme blow-over that may have stalled the rotor during strong current episodes. This did not happen at M4, for which additional buoyancy was added, as the blow-over issue became evident during the summer 2004 cruise. However, the main point that WB of 2003 observed more energetic salty bottom events than M4 of 2004 remains valid, though it is possible that we undercount the salty event speeds if they occur at the times of major blow-over. But as the blow-over is mainly due to the full water-column (barotropic) tidal current that occurs in all months, the seasonal signature of the salty events is preserved. As M4 is $\sim 6 \text{ km}$ to the east of WB, caution is advised in interpreting the differences as interannual temporal variability as the effects of spatial variability cannot be ruled out.

A map view of the cold/salty events (Fig. 19) provides a regional view of the Drygalski plume, the westward-veering path of which is indicated by the higher percentage of cold salty HSSW events.

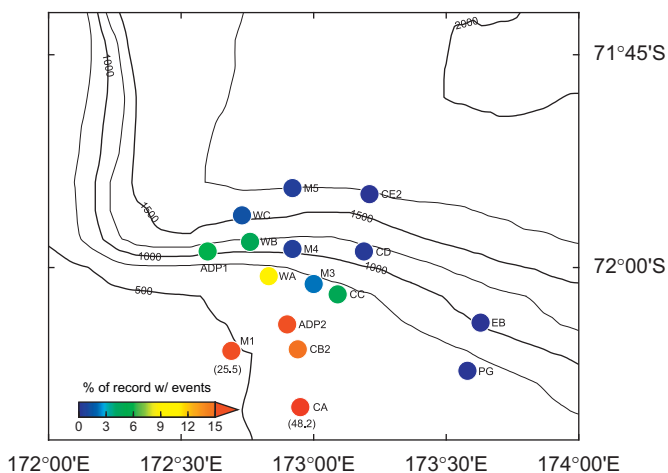


Fig. 19. Percentage of cold salty $\theta < -1^\circ\text{C}$; $S \geq 34.75$ events observed by 30-min sample rate near the sea floor at the AnSlope moorings (Fig. 5 and Table 1).

8. Conclusions

We describe the regional stratification and velocity characteristics of the energetic gravity currents observed over the continental slope of the western Ross Sea during the AnSlope and CLIMA cruises in 2003 and 2004, and with 2 years of currents, temperature, and salinity time series obtained by the AnSlope moorings. The key findings are as follows:

- The most energetic gravity currents observed over the western continental slope of the Ross Sea are derived from export of the High Salinity Shelf Water. The properties of the benthic layer over the continental slope are governed by access to shelf water via three primary deep north–south troughs on the continental shelf and by subsequent mixing enhanced by regionally strong tides (Whitworth and Orsi, 2006; Muench et al., 2008; Padman et al., 2009). The 34.7 isohaline, which may be taken to represent the upper stratum of HSSW, slopes to greater depths towards the east, allowing HSSW as salty as 34.82 to be exported directly into the open ocean via the Drygalski Trough, the westernmost of the three major troughs. The Glomar Challenger Trough farthest east does not provide access of HSSW saltier than 34.72 to the slope, while the Joides Trough offers an escape route for HSSW having an intermediate salinity of up to 34.78. The ISW ($T < -1.9^\circ\text{C}$), formed at the main Ross Ice Shelf, adds volume flux to the Shelf Water export, and its very low temperature enhances the thermobaric effect and thus may play a central role in determining the final properties of waters that penetrate into the deep ocean.
- The benthic layer rapidly increases in thickness from 100 to 400 m as the water depth increases from 600 to 1200 m. Over this interval the bottom water (detided) descends at a mean angle to the local isobaths of $\sim 40^\circ$ and occasionally higher. Benthic layer thickness of 400–500 m is common from 1200 to 1900 m depths, as the flow turns westward in a more isobath-following path. As the sea floor further deepens the distinct benthic layer gradually loses its identity. The benthic layer is markedly thicker west of the Drygalski Trough, consistent with entrainment and vertical mixing consequent to the more energetic bottom currents associated with the saltier (denser) gravity currents derived from that trough. The scatter of benthic layer thickness as a function of bottom depth may reflect changes in the interaction of the gravity current with the overlying ambient water column. Primary interactions are entrainment leading to increased thickness and detrainment as the integrity of the gravity current disappears at increasing bottom depths.
- The northward transport of benthic water observed in summer 2004 off Cape Adare was $\sim 1.7 \text{ Sv}$. The θ/S properties indicate this flow to be composed of roughly $\sim 25\%$ Ross shelf HSSW, or a HSSW transport of $\sim 0.4 \text{ Sv}$. The mooring time series farther east shows export of HSSW primarily during the 6-month summer–fall period, thus the annual mean benthic layer transport may be $\sim 0.85 \text{ Sv}$ containing 0.2 Sv of HSSW from Drygalski Trough. Smethie and Jacobs (2005) determine a production rate of ISW (formed from HSSW) water of 0.86 Sv . A loss of HSSW by direct export to the deep ocean of 0.2 Sv , derived above, yields an overall HSSW loss of 1.0 Sv , 19% of the circumpolar export of Shelf Water, implying a 2–4 year residence time for HSSW. This should be considered however as a lower bound, as there is likely some direct export of HSSW outside of the Cape Adare path, e.g. via the more eastern route offered by Glomar Challenger Trough directly into the Southeast Pacific Basin. Additionally, HSSW export in summer–fall 2003 may have been enhanced due to the presence of the

large iceberg C-19 (see http://www.nasa.gov/vision/earth/environment/iceberg_C-19.html), leading to a lower residence time than may be the norm. A decadal scale reduction in HSSW salinity (Jacobs et al., 2002) may impose a longer temporal element to the HSSW export.

- The time series of bottom-water potential temperature and salinity over the continental slope measured by mooring WB at 1014 m show many episodic, cold ($< -1\text{ }^{\circ}\text{C}$), salty (> 34.75) bottom-water events, which correlate with strong bottom currents. The downhill descent angle of these events increases with bottom-water salinity, reaching $\sim 60^{\circ}$ to the local isobaths when the percentage of HSSW reaches $\sim 100\%$ ($-1.9\text{ }^{\circ}\text{C}$; 34.79). This in turn suggests a rapid descent from the outer shelf to the 1000 m isobath, during which only minimal mixing is possible with ambient slope water. At the sea floor (971 m) at mooring EB, 30 km east of WB, there were few if any HSSW outbreaks, consistent with sharp westward veering of the Drygalski plume in response to the Coriolis force upon its descent over the upper continental slope.
- A histogram of cold ($\leq -1\text{ }^{\circ}\text{C}$) salty (≥ 34.75) outflow events over a two-year time period was constructed by combining near-bottom records from moorings WB and M4. In 2004, there was a dramatic reduction in such events around 1 June, suggesting a similar seasonal signal as seen in 2003. However, there were far fewer cold/salty events in the summer of 2003/2004. This result may reflect interannual variability or the 6 km separation of WB and M4, which is a significant distance relative to path and width of the Drygalski plume and exceeds the local radius of deformation.
- The 30-day low-pass time series of bottom water shows a reduction of HSSW export after May 2003, followed by an increase in November 2003. The frequent occurrence of HSSW events during March–May 2003 may be associated with the large iceberg C-19, which remained grounded over the edge of the Drygalski Trough during the AnSlope-1 period until its late May 2003 departure from the Ross Sea, passing over the AnSlope moorings between 13 and 25 May 2003. The coldest, saltiest bottom water was measured from mid-April to mid-May 2003, just prior to the C-19 departure. Large icebergs may act as “Islands” altering the apparent topography and circulation (Grosfeld et al., 2001) as well as the primary productivity (Arrigo and Van Dijken, 2003). We speculate that C-19 may have enabled accelerated export of HSSW in 2003, acting to deplete the HSSW reservoir with consequential reduced export in 2004. The potential effects of C-19 on the circulation and gravity currents of the western Ross Sea are being developed as a separate study.

Our study presents a regional view of gravity currents over the continental slope of the western Ross Sea. However, caution is suggested, as small-scale variability may be substantial within the polar stratification. Submarine canyons and other irregularities of the sea floor may influence benthic stratification, shear, and the path and interaction of the gravity currents with the ambient stratification. Additionally, tidal currents, and eddies along the slope front, may set the timing of the export of dense Shelf Water. All of these factors require further study through models and more specialized observational programs.

Acknowledgments

The AnSlope program was supported by the National Science Foundation (NSF) grants to Lamont-Doherty Earth Observatory of Columbia University OPP 01-25172 for the AnSlope data collection phase, OPP-0440823 and ANT-0538148 for the data analysis

phase; by NSF grants OPP-01256023 and ANT-0440656 to Earth & Space Research; grant N00014-03-1-0067 from the Office of Naval Research to Earth & Space Research; and NSF grants OPP-0125084 and OPP-0440657 to Texas A&M University. Comments from reviewers Keith Nicholls and Andreas Macrander, who deserves special credit for doing the entire review while at sea, were very constructive and have greatly improved the presentation. A. Gordon prepared this manuscript while on a Columbia University sabbatical leave at the Consiglio Nazionale delle Ricerche Istituto di Scienze dell'Atmosfera e Del Clima (ISAC), Tor Vergata, Italy. Rosalia Santoleri, Enrico Zambianchi, Francesco Bignami and Emanuele Böhm made his visit at ISAC both enjoyable and productive. Lamont-Doherty Earth Observatory contribution number 7185; ESR contribution number 95.

References

- Arrigo, K.R., Van Dijken, G., 2003. Impact of iceberg C-19 on Ross Sea primary production. *Geophysical Research Letters* 30 (16).
- Baines, P.G., Condie, S., 1998. Observations and modelling of Antarctic downslope flows. In: Jacobs, S., Weiss, R. (Eds.), *Ocean, Ice and Atmosphere: Interactions at the Antarctic Continental Margin*, vol. 75. Antarctic Research Series, AGU, Washington, DC, pp. 29–49.
- Bergamasco, A., Defendi, V., Zambianchi, E., Spezie, G., 2002. Evidence of dense water outflow on the Ross Sea shelf-break. *Antarctic Science* 14 (3), 271–277.
- Brennecke, W., 1921. Die ozeanographischen Arbeiten der Deutschen Antarktischen Expedition 1911–1912 (“Deutschland”). *Aus dem Archiv der Deutschen Seewarte* 39, 1–216.
- Bromwich, D.H., Kurtz, D.D., 1984. Katabatic wind forcing of the Terra Nova Bay Polynya. *Journal of Geophysical Research* 89, 3561–3572.
- Budillon, G., Spezie, G., 2000. Thermohaline structure and variability in the Terra Nova Bay Polynya, Ross Sea. *Antarctic Science* 12, 493–508.
- Erofeeva, S.Y., Egbert, G.D., Padman, L., 2005. Assimilation of ship-mounted ADCP data for barotropic tides: application to the Ross Sea. *Journal of Atmospheric and Oceanic Technology* 22 (6), 721–734.
- Foldvik, A., Gammelsrød, T., 1988. Notes on southern-ocean hydrography, sea-ice and bottom water formation. *Paleogeography Paleoclimatology Paleoecology* 67, 3–17.
- Foldvik, A., Gammelsrød, T., Østerhus, S., Fahrbach, E., Rohardt, G., Schröder, M., Nicholls, K., Padman, L., Woodgate, R., 2004. Ice Shelf Water overflow and bottom water formation in the southern Weddell Sea. *Journal of Geophysical Research* 109, C02015.
- Foster, T., 1995. Abyssal water formation off Wilkes Land coast of Antarctica. *Deep-Sea Research* 42, 501–522.
- Foster, T., Carmack, E., 1976a. Frontal zone mixing and Antarctic Bottom Water formation in the southern Weddell Sea. *Deep-Sea Research* 23, 301–317.
- Foster, T., Carmack, E., 1976b. Temperature and salinity structure in the Weddell Sea. *Journal of Physical Oceanography* 6, 36–44.
- Gill, A.E., 1973. Circulation and bottom water formation in the Weddell Sea. *Deep-Sea Research* 20, 111–140.
- Girton, J.B., Sanford, T.B., 2003. Descent and modification of the overflow plume in the Denmark Strait. *Journal of Physical Oceanography* 33, 1351–1363.
- Gordon, A.L., 1966. Potential temperature, oxygen and circulation of bottom water in the Southern Ocean. *Deep-Sea Research* 13, 1125–1138.
- Gordon, A.L., 1974. Varieties and variability of Antarctic bottom water. In: *Processus de Formation des Eaux Oceaniques Profondes (en particulier en Mediterranee Occidentale)*. Editions du Centre National de la Recherche Scientifique, Paris, France, No. 215, pp. 33–47.
- Gordon, A.L., 1998. Western Weddell Sea thermohaline stratification. In: Jacobs, S.S., Weiss, R.F. (Eds.), *Ocean, Ice and Atmosphere: Interactions at the Antarctic Continental Margin*, vol. 75. American Geophysical Union, Washington, DC, pp. 215–240.
- Gordon, A.L., Zambianchi, E., Orsi, A., Visbeck, M., Giulivi, C., Whitworth III, T., Spezie, G., 2004. Energetic plumes over the western Ross Sea continental slope. *Geophysical Research Letters* 31, L21302.
- Grosfeld, K., Schroder, M., Fahrbach, E., Gerdes, R., Mackensen, A., 2001. How iceberg calving and grounding change the circulation and hydrography in the Filchner Ice Shelf-Ocean system. *Journal of Geophysical Research* 106, 9039–9056.
- Ivanov, V., Shapiro, G., Huthnance, J., Aleynik, D., Golovin, P., 2004. Cascades of dense water around the world ocean. *Progress in Oceanography* 60, 47–98.
- Jacobs, S.S., 1991. On the nature and significance of the Antarctic Slope Front. *Marine Chemistry* 35, 9–24.
- Jacobs, S.S., 2004. Bottom water production and its links with the thermohaline circulation. *Antarctic Science* 16, 427–437.
- Jacobs, S.S., Amos, A.F., Bruchhausen, P.M., 1970. Ross Sea oceanography and Antarctic Bottom Water formation. *Deep-Sea Research* 17, 935–962.
- Jacobs, S.S., Fairbanks, R.G., Horibe, Y., 1985. Origin and evolution of water masses near the Antarctic continental margin: evidence from $\text{H}_2^{18}\text{O}/\text{H}_2^{16}\text{O}$ ratios in sea

- water. In: Jacobs, S.S. (Ed.), *Oceanology of the Antarctic Continental Shelf*, Antarctic Research Series, vol. 43. AGU, Washington, DC, pp. 59–85.
- Jacobs, S.S., Giulivi, C.F., Mele, P., 2002. Freshening of the Ross Sea during the late 20th century. *Science* 297, 386–389.
- Johnson, G.C., 2008. Quantifying Antarctic Bottom Water and North Atlantic Deep Water volumes. *Journal of Geophysical Research* 113, C05027.
- Kurtz, D.D., Bromwich, D.H., 1983. Satellite observed behavior of the Terra Nova Bay Polynya. *Journal of Geophysical Research* 88, 9717–9722.
- Kurtz, D.D., Bromwich, D.H., 1985. A recurring, atmospherically forced Polynya in Terra Nova Bay. In: Jacobs, S.S. (Ed.), *Oceanology of the Antarctic Continental Shelf*. American Geophysical Union, Washington, DC, pp. 177–201.
- LeBel, D.A., Smethie Jr., W.M., Rhein, M., Kieke, D., Fine, R.A., Bullister, J.L., Min, D.-H., Roether, W., Weiss, R.F., Andri , C., Smythe-Wright, D., Peter Jones, E., 2008. The formation rate of North Atlantic Deep Water and Eighteen Degree Water calculated from CFC-11 inventories observed during WOCE. *Deep-Sea Research Part I: Oceanographic Research Papers* 55, 891–910.
- Legg, S., Chang, Y., Chassignet, E., Danabasoglu, G., Ezer, T., Gordon, A., Griffes, S., Hallberg, R., Jackson, L., Large, W., Ozgokmen, T., Peters, H., Price, J., Riemenschneider, U., Wu, W., Xu, X., Yang, J., 2009. Improving oceanic overflow representation in climate models: the Gravity Current Entrainment Climate Process Team. *Bulletin of the American Meteorological Society*, in press.
- Lusquinos, A.J., 1963. Extreme temperatures in the Weddell Sea. *Arbok University Bergen Matematisk Naturvitenskapelig Serie* 23, 1–19.
- McDougall, T.J., 1987. Thermobaricity, cabling and watermass conversion. *Journal of Geophysical Research* 92, 5448–5464.
- McPhee, M., 2003. Is thermobaricity a major factor in Southern Ocean ventilation? *Antarctic Science* 15(1), 153–160 (doi:10.1017/S0954102003001159).
- Mosby, H., 1934. The water of the Atlantic Antarctic Ocean. *Scientific Results of the Norwegian Antarctic Expedition 1927–1928* (1), 131.
- Muench, R.D., Padman, L., Gordon, A.L., Orsi, A.H., 2008. Mixing of a dense water outflow from the Ross Sea, Antarctica: the contribution of tides. *Journal of Marine Systems* [doi:10.1016/j.jmarsys.2008.11.003].
- Orsi, A.H., Whitworth III, T., 2004. Hydrographic Atlas of the World Ocean Circulation Experiment (WOCE). In: Sparrow, M., Chapman, P., Gould, J. (Eds.), Volume 1: Southern Ocean. International WOCE Project Office, Southampton, UK.
- Orsi, A.H., Johnson, G.C., Bullister, J.L., 1999. Circulation, mixing, and production of Antarctic Bottom Water. *Progress in Oceanography* 43, 55–109.
- Orsi, A.H., Jacobs, S.S., Gordon, A.L., Visbeck, M., 2001. Cooling and ventilating the Abyssal Ocean. *Geophysical Research Letters* 28 (15), 2923–2926.
- Orsi, A.H., Smethie Jr., W.M., Bullister, J.L., 2002. On the total input of Antarctic Waters to the Deep Ocean: a preliminary estimate from chlorofluorocarbon measurements. *Journal of Geophysical Research* 12, 12.
- Orsi, A.H., Wiederwohl, C.L., 2009. A recount of Ross Sea waters. In: Gordon, A., Padman, L., Bergamasco, A. (Eds.), *Deep-Sea Research Part II, Southern Ocean Shelf Slope Exchange*, this issue [doi:10.1016/j.dsr2.2008.10.033].
- Ou, H.-W., 2005. Dynamics of dense water descending a continental slope. *Journal of Physical Oceanography* 35, 1318–1328.
- Özgökmen, T., Fisher, P., Duan, J., Iliescu, T., 2004. Entrainment in bottom gravity currents over complex topography from three-dimensional nonhydrostatic simulations. *Geophysical Research Letters* 31, L13212.
- Padman, L., Erofeeva, S., Joughin, I., 2003. Tides of the Ross Sea and Ross Ice Shelf cavity. *Antarctic Science* 15, 31–40 (doi:10.1017/S0954102003001032).
- Padman, L., Howard, S., Orsi, A., Muench, R., 2009. Tides of the Northwestern Ross Sea and their impact on dense outflows of high salinity shelf water. In: Gordon, A., Padman, L., Bergamasco, A. (Eds.), *Deep-Sea Research Part II, Southern Ocean Shelf Slope Exchange*, this issue [doi:10.1016/j.dsr2.2008.10.026].
- Peters, H., Johns, W.E., Bower, A.S., Fratantoni, D.M., 2005. Mixing and entrainment in the Red Sea outflow plume. Part I: plume structure. *Journal of Physical Oceanography* 35, 569–583.
- Price, J.F., Baringer, M.O., 1994. Outflows and deep-water production by Marginal Seas. *Progress in Oceanography* 33 (3), 161–200.
- Price, J.F., Baringer, M.O., Lueck, R.G., Johnson, G.C., Ambar, I., Parrilla, G., Cantos, A., Kennelly, M., Sanford, T., 1993. Mediterranean outflow mixing and dynamics. *Science* 259, 1277–1282.
- Rintoul, S.R., 1998. On the origin and influence of Adelie Land Bottom Water. In: Jacobs, S., Weiss, R. (Eds.), *Ocean, Ice and Atmosphere: Interactions at the Antarctic Continental Margin*. Antarctic Research Series, vol. 75. American Geophysical Union, Washington, DC, pp. 151–171.
- Saunders, P.M., 1990. Cold Outflow from the Faroe Bank Channel. *Journal of Physical Oceanography* 20, 29–43.
- Smethie, W.M., Fine, R.A., 2001. Rates of North Atlantic Deep Water formation calculated from chlorofluorocarbon inventories. *Deep-Sea Research I* 48 (1), 189–215.
- Smethie Jr., W.M., Jacobs, S.S., 2005. Circulation and melting under the Ross Ice Shelf: estimates from evolving CFC, salinity and temperature fields in the Ross Sea. *Deep-Sea Research I* 52, 959–978.
- Smith, W.H.F., Sandwell, D.T., 1997. Global seafloor topography from satellite altimetry and ship depth soundings. *Science* 277, 1957–1962.
- Tanaka, K., Akitomo, K., 2001. Baroclinic instability of density current along a sloping bottom and the associated transport process. *Journal of Geophysical Research* 106 (C2), 2621–2638.
- Van Woert, M.L., 1999. Wintertime dynamics of the Terra Nova Bay Polynya. *Journal of Geophysical Research* 104, 7753–7769.
- Visbeck, M., Thurnherr, A.M., 2009. High-resolution velocity and hydrographic observations of the Drygalski Trough Gravity Plume. In: Gordon, A., Padman, L., Bergamasco, A. (Eds.), *Deep-Sea Research Part II, Southern Ocean Shelf Slope Exchange*, this issue [doi:10.1016/j.dsr2.2008.10.029].
- Whitworth, T., Orsi, A.H., 2006. Antarctic Bottom Water production and export by tides in the Ross Sea. *Geophysical Research Letters* 33 (12), 1–4.
- Whitworth, T., Orsi, A.H., Kim, S.-J., Nowlin Jr., W.D., 1998. Water masses and mixing near the Antarctic Slope Front. In: Jacobs, S.S., Weiss, R.F. (Eds.), *Ocean, Ice, and Atmosphere: Interactions at the Antarctic Continental Margin*. American Geophysical Union, Washington, DC, pp. 1–27.
- Xu, X., Chang, Y., Peters, H., Özgökmen, T., Chassignet, E., 2006. Parameterization of gravity current entrainment for ocean circulation models using a high-order 3D nonhydrostatic spectral element model. *Ocean Modelling* 14, 19–44.